Quantized Hall effect and quantum phase transitions in coupled two-layer electron systems

Song He*
Department of Physics, University of Maryland, College Park, Maryland 20742

S. Das Sarma
Institute for Theoretical Physics, University of California, Santa Barbara, California 93106
and Department of Physics, University of Maryland, College Park, Maryland 20742†

X. C. Xie‡
Department of Physics, University of Maryland, College Park, Maryland 20742
(Received 23 September 1992)

We study the nature of the many-body electron states (and quantum phase transitions between them) in a double-quantum-well structure under a strong external magnetic field as a function of the materials parameters that define the two-layer system, namely, the thickness of individual layers, the separation between them, the individual well potentials confining the electrons, and the potential barrier between them. Motivated by two recent experiments, we consider two different situations, one with (almost) no quantum tunneling between the wells, and the other with substantial interwell quantum tunneling. We use the spherical system finite-size exact diagonalization technique for our calculations. By calculating the overlap of our exact small-system numerical wave functions with various (postulated) analytic wave functions, we comment on the nature of the incompressibility for various Landau-level filling factors (ν). We investigate, in particular details, the possibility of $\nu=\frac{1}{2}$ (i.e., $\frac{1}{4}$ average occupancy in each well), and, 1 (i.e., $\frac{1}{2}$ occupancy in each well) incompressible states where ν is the total filling factor for the system. We also provide results for the $\nu=\frac{2}{3}$ situation. Our conclusion, based on our use of realistic system parameters in our calculations, is that in both the recent experimental realizations of the $\nu=\frac{1}{2}$ fractional quantum Hall effect, the relevant ground state is the so-called 331 state which is stabilized by the competition between intrawell and interwell electron-electron correlations. We calculate for various double-quantum-well structural parameters and magnetic fields the $\nu=\frac{1}{2}$ excitation spectra and the energy gaps, and compare it with the recent experimental data, obtaining excellent quantitative agreement. We provide a detailed quantum phase diagram for the $\nu=1$ state as a function of the interwell Coulomb interaction and the symmetric-antisymmetric single-particle gap, and find that the $\nu=1$ quantum Hall effect observed in the two recent experiments, in contrast to the $\nu=\frac{1}{2}$ effect, belongs in some sense to two different universality classes. We also predict the existence of a reentrant $\nu=1$ quantum Hall effect in double-quantum-well systems.

I. INTRODUCTION

Laughlin's theory[1] for the fractional quantum Hall effect[2] (FQHE) is based on the following Jastrow-type many-particle wave function:

$$\psi_m(u_1,\ldots,u_N)=\prod_{i<j}(u_i-u_j)^m\exp\left[-\tfrac{1}{4}\sum_{j=1}^{N}|u_j|^2\right] \quad (1)$$

for the ground state. Here, $u_j=x_j-iy_j$ is the complex representation for the two-dimensional (2D) coordinates (x_j,y_j) of the jth electron, $m=\nu^{-1}$ is an odd integer where ν is the filling factor, $\nu=eB/(chN)$ with B the perpendicular magnetic field, and N the 2D electron density. Throughout this paper we neglect any explicit consideration of electron spin assuming that the magnetic-field B is always high enough to totally spin polarize the system due to a large Zeeman splitting and our interest is in the lowest spin-split state. We also ignore any effects of Landau-level mixing and higher subbands, working exclusively in the lowest spin-split Landau level of the lowest subband. (All the experimental work to be discussed and compared with our theory in this paper satisfies these conditions.) Laughlin's wave function describes an incompressible liquid state at the magic filling factors $\nu=m^{-1}=\frac{1}{3},\frac{1}{5},\frac{1}{7},\ldots$, where the system develops an excitation gap separating the ground state from the excited states. The ground-state energy itself has cusps at these primary fractional fillings $\nu=\frac{1}{3},\frac{1}{5}$, etc., which (once one invokes some mechanism, such as localization, to allow the chemical potential to move smoothly through the excitation gap) is sufficient[3,4] to produce FQHE. The theory was later generalized[3-7] to include other fractional states of the form $\nu=p/q$ with q odd (e.g., $\nu=\frac{2}{5},\frac{3}{7}$, etc.). The essential theory based on the wave function described by Eq. (1) is universally accepted (and, has been verified in many direct numerical calculations) to be the theoretical explanation for the FQHE in a single-layer 2D system.

The key element in the physics of the FQHE is the in-

compressibility (equivalently, the excitation gap or the cusp in the ground-state energy as a function of ν) induced by short-range correlations due to electron-electron interaction. The integral quantum Hall effect (IQHE) phenomenon[8] is also due to incompressible states at integer $\nu=1,2,3,\ldots$, which, however, arise not from electron correlation effects, but from the excitation gaps associated with the quantization of the noninteracting kinetic energy into distinct Landau levels. The angular-momentum quantum number m in Eq. (1) is necessarily an odd integer due to the needed antisymmetry of the fermion wave function arising from the Fermi statistics. Thus, the incompressibility of the FQHE state arising from short-range electron correlations exists only at odd denominator fractional fillings $\nu=m^{-1}$, immediately "explaining" the early puzzle of why the FQHE does not happen at even denominator fractions (e.g., $\nu=\frac{1}{2}$).

Following Laughlin's work, Halperin pointed out[4] that it should be possible to observe even fractional states $\nu=p/q$ with q an even integer, provided one considers a multicomponent 2D electron system where electrons carry (at least) one additional quantum index associated with some other (i.e., in addition to the orbital motion) degrees of freedom. Specifically, the introduction of spin degrees of freedom into the problem (explicitly ignored in our discussion and in Laughlin's original work) would, in principle, allow the possibility of even denominator fractions where states of mixed spin polarization can exist where two or more orbital Landau levels are nearly degenerate. Because of the small g factor in GaAs, the most obvious possibility for the realization of such a multicomponent 2D system occurs in a weak magnetic field where the Zeeman splitting is small, making the spin degrees of freedom relevant. The incompressibility responsible for the FQH state arises from there being a maximum filling factor at which the possibility of any pair of electrons being in a state of some low relative angular momentum can be avoided. In the absence of any Zeeman energy, electrons can gain considerable correlation energy by reversing half of their spins. In the presence of Zeeman energy, it becomes a quantitative question whether reversed spin states can be incompressible ground states for some even denominator fractions at weak enough magnetic fields. This issue has been addressed in detail[9-11] in the theoretical literature. In fact, it has been suggested[10,11] that the weak $\nu=\frac{5}{2}$ FQHE originally observed[12] by Willett *et al.* in a tilted magnetic-field experiment is such a spin-singlet ground state. Thus, the odd denominator rule for the FQHE can be relaxed by introducing new quantum numbers associated with additional degrees of freedom. We will not discuss these spin-unpolarized (or, partially polarized) states any more except to mention that there is substantial theoretical literature[9-11] on the subject and quite a few puzzling experimental observations[12,13] in higher Landau levels (i.e., $\nu>1$) have been interpreted using spin generalizations of the Laughlin state. Our reason for mentioning the mixed spin states is to point out that, in the presence of new degrees of freedom, it is possible to relax the odd denominator requirement of the original Laughlin incompressible state because the antisymmetry requirement of the wave function is more complicated than that in Eq. (1) in the presence of additional quantum numbers.

In this paper, we provide a detailed quantitative theoretical study of FQHE states in a two-component 2D quantum plasma where the additional degree of freedom arises from having two parallel 2D electron layers which are separated by a distance in the third (z) direction. Two-layer (or, more generally, multilayer) structures have attracted considerable attention over the years both theoretically[14] and experimentally[15] for their electronic properties, particularly in the context of plasmon dispersion studies[14,15] in low-dimensional systems. These double-layer structures are clearly well suited for studying generalized incompressible states in a two-component strongly correlated 2D system. While there is much superficial similarity between the two-spin and the two-layer systems (in fact, one can think of the layer index as a pseudospin index[16] to emphasize this formal similarity), there are significant differences as well. In the spin problem the electron-electron interaction is spin independent (i.e., Coulomb interaction between two electrons is the same for spin up and spin down) while in the layer problem the interaction is pseudospin dependent because the intralayer and interlayer interactions are obviously different. Thus, in the spin problem the system wave functions must be eigenstates of both the total spin and the z component of the spin angular momentum, whereas in the layer problem neither the total pseudospin nor its z component (in the presence of tunneling between the layers) is conserved. In the absence of any actual interlayer electron hopping or tunneling, the z component of the pseudospin is conserved in the double-layer problem, but the total pseudospin is still unconserved because it does not commute with the Hamiltonian which is now pseudospin (i.e., layer) dependent.

The model for the double-quantum-well (DQW) system considered (Fig. 1) in this paper consists of two identical finite-width (with an individual well width in the z direction denoted by D_w) square quantum wells separated by a barrier of width D_b. The center-to-center distance or the well separation (d) between the two wells in the z direction is, therefore, $d=D_w+D_b$. We model each well of the DQW structure by a finite "asymmetric" square-well potential of depth V_w (and of width D_w) and the potential barrier separating them be a square barrier of height V_b (and of width D_b). For $V_w=V_b$, a situation we study in

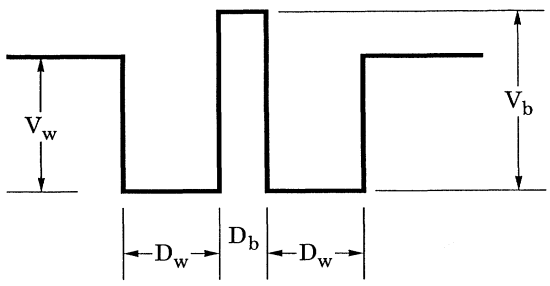

FIG. 1. Shows the schematic potential diagram for the DQW structure used in the calculations.

some detail, each well becomes a symmetric finite square well. The materials parameters for the DQW structure in our calculations are, therefore, D_w, D_b, V_w, and V_b. We assume a symmetric or balanced situation with equal electron density $N/2$ in each well with a total density of N. In addition to these four independent materials parameters (or three, if $V_w = V_b$) defining the DQW itself, there is an additional length (or energy) parameter associated with the intrawell Coulomb interaction, given by the magnetic length or the cyclotron radius $l_c = (c\hbar/eB)^{1/2}$ with the intrawell Coulomb correlation energy being of the order of $e^2/\varepsilon l_c$ for each well, where ε is the background lattice dielectric constant. When the interlayer Coulomb interaction energy, given approximately by $e^2/2\varepsilon d$, is comparable to the intralayer correlation energy, i.e., when $l_c \sim d/2$, one expects a new ground state for the system. For $d \ll l_c$, the system behaves as a *single* 2D layer with a filling factor ν whereas for $d \gg l_c$ the DQW system consists of two *isolated* 2D layers each with a fractional filling of $\nu/2$. Our main interest is in investigating the possible (experimentally realizable) existence of incompressible FQH states for intermediate values of the DQW separation d.

The qualitative discussion[17] given above, where one expects some incompressible ground state for $d \sim 2l_c$, is based[17] on there being no other length scale in the problem (i.e., in addition to d and l_c). But, in reality (and in our *realistic* model as well), there is an additional length scale $\lambda \sim D_w$ defining the width or the thickness of each 2D layer in the DQW structure. Obviously, λ softens the intralayer Coulomb correlation[18]—in fact, it is possible to completely destroy[19,20] the incompressibility by increasing λ which preferentially enhances the relative contribution of the long-range part of the Coulomb interaction compared to the short-range part. Thus, in real systems, due to the finite thickness of each electron layer, the approximate equality of the intralayer and correlations occurs at a larger value of the interwell separation $d \sim 2(l_c^2+\lambda^2)^{.1/2}$ Another complication in real systems is the presence of interwell electron tunneling due to the overlap of the z wave function in the individual wells. In the presence of tunneling, the z component of the pseudospin is not conserved. Clearly, for small enough values of d (and, for a finite barrier height V_b), tunneling is quantitatively significant and must be included in the theoretical calculation. As the well separation d (or V_b) increases, tunneling is exponentially suppressed and our simple qualitative consideration applies. Tunneling introduces another energy scale Δ_{sas}, the so-called symmetric-antisymmetric energy gap, in the problem—Δ_{sas} is the energy splitting between the 2D subbands in the two wells (which are degenerate in the absence of tunneling) due to the overlap of the z wave functions. For large Δ_{sas}, the FQH states are destroyed. (We find that for small values of Δ_{sas}, the $\nu = \frac{1}{2}$ FQHE is quite robust and survives the effect of interwell tunneling.)

The first systematic investigation of possible FQHE in DQW structures was carried out[21] by Yoshioka, MacDonald, and Girvin following an earlier suggestion[16] by Haldane and Rezayi mentioning the possibility of interesting FQH states in DQW structures. An early numerical study on a DQW structure using rectangular geometry was also carried out in Ref. 22 for the $\nu = 1$ situation, suggesting the possibility of an incompressible state where each *individual* layer has a filling factor of $\frac{1}{2}$. In all of these references,[16,21,22] a highly idealized DQW model was used in which each well is taken to be a purely δ-function-like ideal 2D layer with zero thickness. Thus, the model is characterized by only two length scales, the layer separation d and the magnetic length l_c with the physics of finite layer thickness and interwell tunneling both neglected completely. Using a finite-size diagonalization study, Yoshioka, MacDonald, and Girvin investigated[21] the nature of the ground state as a function of d/l_c for $\nu = 1$, $\frac{1}{2}$, $\frac{2}{5}$, and $\frac{1}{3}$. In particular, the possible existence of a $\nu = \frac{1}{2}$ FQHE in a DQW structure around $d/l_c \sim 2$ was pointed out in Ref. 21. Our primary interest in this work is to investigate, in detail, the possible realization of FQH states in *realistic* DQW structures—we are, therefore, mainly interested in the $\nu = \frac{1}{2}$ situation which does *not* occur in single 2D layers. We present some results for $\nu = 1$ as well—of course, $\nu = 1$ QHE regularly occurs in a 2D system, however, for a DQW structure $\nu = 1$ implies that the average filling factor is $\frac{1}{2}$ in each layer. Our most important difference with the earlier theoretical work[16,21,22] on DQW systems is our use of a realistic model with finite well widths and finite interwell tunneling in contrast to the ideal systems studied in Refs. 21 and 22. Using realistic values of D_w, D_b, V_w, and V_b (as we do) in the theoretical model has turned out to be crucial in the experimental design of the DQW structures for the eventual realization of the $\nu = \frac{1}{2}$ FQHE. In fact, our calculations[23,24] were used by the experimentalists in making the optimum choice for the materials parameters[25] (i.e., V_w, V_b, D_w, D_b) of the DQW structures for the eventual observation of the $\nu = \frac{1}{2}$ FQHE. Neglect of finite layer widths and the well and barrier potentials in the ideal model[21] makes it quantitatively unsuitable to be compared with the experimental[25,26] results. The actual feasibility of observing the $\nu = \frac{1}{2}$ FQHE in a DQW structure was, however, qualitatively established by these idealized calculations.[21]

The predicted[21,23,24] $\nu = \frac{1}{2}$ FQHE in DQW systems has recently been observed[25,26] by two different groups, using DQW structures which are quite different in their structural details. In the study[25] by Eisenstein *et al.*, carried out at AT&T Bell Laboratories, the sample is a traditional symmetric DQW structure (Fig. 2) with $V_w = V_b$, whereas in the work[26] of Suen *et al.*, carried out at Princeton University, the sample is actually a wide *single* quantum well where the self-consistent electric field[27] arising from the presence of the electrons themselves splits the well (Fig. 3) into two spatially separated (in the z direction) electron layers, effectively creating a DQW structure. Thus, even though the bare potential looks substantially different in the two cases, the real self-consistent potentials are not that different, and, in fact, the electron charge-density profiles (in the z direction) in the two cases (Figs. 2 and 3) are qualitatively similar. Based on the fact that the experimental sample of Ref. 26 is a single quantum well, it has recently been argued[28]

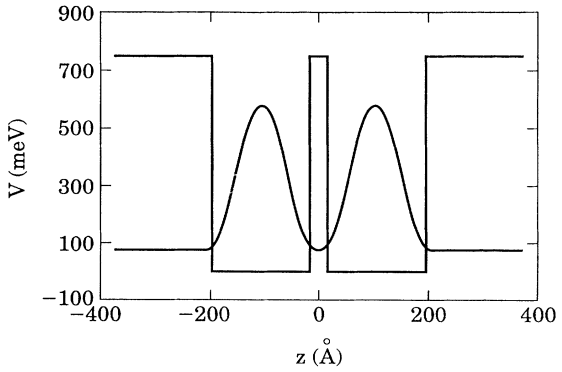

FIG. 2. The DQW structure corresponding to Ref. 25 (AT&T samples) used in the calculations. $V_w = V_b = 750$ meV; $D_w = 120$ or 180 Å; $D_b = 51$ and 31 Å (samples *A*, *B*, and *C*), and 99 Å (sample *D*). The electron charge density is also shown.

that the $\nu = \frac{1}{2}$ FQHE observed[26] in the Princeton sample is *qualitatively different* from that observed in Ref. 25 (i.e., they belong to different universality class), because the presence of tunneling in Ref. 26 makes the electron species in the two layers essentially indistinguishable whereas the more conventional DQW system of Ref. 25 with a high potential barrier (and, therefore, little tunneling) represents the standard theoretical model[16,21] of two distinguishable species. We disagree with this viewpoint[28] and believe that the $\nu = \frac{1}{2}$ FQHE states observed in Refs. 25 and 26 are qualitatively the same ground state (namely, the 331 state first proposed[4] by Halperin) and we present numerical evidence that this state is quite robust and survives some interwell tunneling.[23,24] In fact, our numerical calculations using the actual materials parameters of the Princeton sample[26] show the $\nu = \frac{1}{2}$ FQHE in Ref. 26 to have the same 331 ground

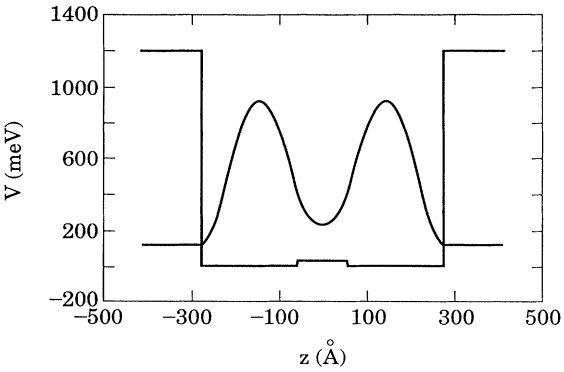

FIG. 3. The DQW structure corresponding to Ref. 26 (Princeton sample) used in the calculations. The real structure is a wide single quantum well where self-consistency effects produce an effective double-layer structure. The effective parameters ($V_w = 1.2$ eV; $V_b = 25$ meV; $D_w = 220$ Å; $D_b = 120$ Å) used in our calculations are such that the correct self-consistent charge density (also shown) and the Δ_{sas} ($= 0.97$ meV) are reproduced.

state as the AT&T sample.[25] We will present these results later in this article, establishing that the $\nu = \frac{1}{2}$ FQH states observed in Refs. 25 and 26 are in the same universality class. We believe that the *bare* Δ_{sas}, which is quite large (~ 10 K) in Ref. 26, is *not* the relevant parameter determining the nature of the ground state in the strongly correlated system. Electron-electron interaction strongly affects the single-particle tunneling by broadening the individual symmetric or antisymmetric single-particle states (in fact, for strong enough interwell Coulomb interaction the single-particle tunneling gap vanishes), and the correct parameter determining the nature of the correlated ground state is the *renormalized* Δ_{sas}. Our direct numerical calculations suggest that the renormalized Δ_{sas} in Ref. 26 is small and the ground state is the 331 state which is exact in the limit of vanishing tunneling.

It may be worthwhile to discuss qualitatively[17] the two experimental results[25,26] in light of this apparent difference between the two samples. In Fig. 4, we reproduce the main results of the two experiments, both clearly showing the $\nu = \frac{1}{2}$ FQHE. (One can also see many other known integral and fractional QHE's of comparable strengths in the plots of Fig. 4, demonstrating that the $\nu = \frac{1}{2}$ FQHE in DQW systems is a strong, primary effect and *not* a small detail.) The $\nu = \frac{1}{2}$ FQHE in the two cases can be seen to be quite similar qualitatively. There is a substantial quantitative difference between the two experiments in terms of the d/l_c values at which the $\nu = \frac{1}{2}$ FQHE shows up in the two experiments. In Ref. 25, consistent with the earlier theoretical expectations and predictions,[23] the $\nu = \frac{1}{2}$ FQHE occurs around $d/l_c \sim 3$, and is clearly absent for $d/l_c \gtrsim 4$. In Ref. 26, on the other hand, the $\nu = \frac{1}{2}$ FQHE occurs for $d/l_c \sim 7$. This large difference can be understood on the basis of our earlier qualitative discussion including the effect of finite layer width. The effective layer width for the Princeton sample[26] is quite large, $\lambda \sim 3l_c$, whereas in the AT&T sample[25] the layer width is smaller, $\lambda \sim l_c$. Taking into account the softening[18,19] of the intrawell Coulomb correlation energy by the finite layer thickness effect, it is easy to see that the condition of the approximate equality of the intrawell and interwell Coulomb interaction energies, which is needed to stabilize the $\nu = \frac{1}{2}$ FQHE, will occur at much larger relative values of $d(\sim 2[l_c^2 + \lambda^2]^{1/2})$ for the sample of Ref. 26 than that for Ref. 25. Even though the bare tunneling effect is larger in the sample of Ref. 26 ($\Delta_{sas} \sim 0.97$ meV) compared with that of Ref. 25 ($\Delta_{sas} \sim 0.14$ meV), it is a small effect in both, and the same robust $\nu = \frac{1}{2}$ FQH state (i.e., the 331 state of Halperin[4]) is the ground state in both samples. This conclusion is borne out by our detailed numerical calculations.

While our main goal in this paper is to study in detail the $\nu = \frac{1}{2}$ FQHE in DQW structures, we discuss some numerical results for the $\nu = 1$ FQHE as well. One can clearly see the $\nu = 1$ FQHE in the data (Fig. 4) of Refs. 25 and 26. As a function of the interwell separation d (with fixed ν), the $\nu = \frac{1}{2}$ and $\nu = 1$ FQHE have a qualitative difference with respect to the comparative roles of Δ_{sas}, the interwell electron tunneling effect, and the interwell

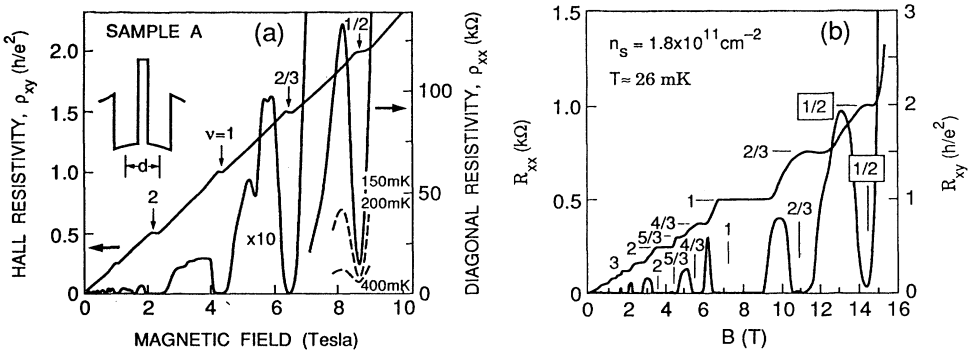

FIG. 4. Shows the DQW experimental QHE data for Ref. 25 (a) and Ref. 26 (b). The $\nu=\frac{1}{2}$, $\frac{2}{3}$, and 1. QHE can clearly be seen in both experiments.

Coulomb interaction energy. As $d\rightarrow 0$, $\nu=\frac{1}{2}$ FQHE is necessarily destroyed, because the single-layer 2D system is compressible at $\nu=\frac{1}{2}$. The $\nu=1$ QHE in a DQW system, on the other hand, is the strongest in the $d\rightarrow 0$ limit. Thus, Δ_{sas} always hinders the $\nu=\frac{1}{2}$ FQHE in a DQW whereas the $\nu=1$ QHE is stabilized by Δ_{sas} in the small-d limit. As d increases, an exponential decrease in Δ_{sas} eventually destroys[29,30] the regular $\nu=1$ QHE. Curiously enough, however, there is a possible *many-body* $\nu=1$ QHE which may exist even for $\Delta_{sas}=0$. In particular, for d large enough so that the intrawell and interwell Coulomb correlation energies are comparable, i.e., for $d\approx 2l_c$ (for a zero well-width model), the so-called 111 many-body state[31] which exhibits $\nu=1$ FQHE may be stabilized even when $\Delta_{sas}=0$ (in fact, finite values of Δ_{sas} hinder this 111 state, just as it does the $\nu=\frac{1}{2}$ 331 state). Thus, the $\nu=1$ effect in a DQW structure can arise from two different physical origins—one, the usual single-particle QHE, is stabilized by the symmetric-antisymmetric gap for large Δ_{sas} (and, therefore, small d) and, the other, a many-body QHE, is stabilized by a many-body gap at small values of Δ_{sas}. Note that for large d, the $\nu=1$ DQW system splits into two isolated 2D layers, each with $\nu=\frac{1}{2}$ showing no FQHE. The destruction of the odd-integral QHE by the relative decrease of Δ_{sas} has been experimentally observed[29,30] recently.

Coming back to the data of Refs. 25 and 26, we believe that *there is a qualitative difference between these two experiments* with respect to their observation of the $\nu=1$ QHE. We believe (and our numerical results strongly suggest) that the $\nu=1$ QHE observed in Ref. 25 corresponds to the 111 many-body ground state whereas that in Ref. 26 corresponds to the finite Δ_{sas} stabilized single-particle ground state. Thus, the $\nu=1$ QHE in the two experiments belong to different universality classes. While this conclusion is based on our finite-size diagonalization numerical results, we make some qualitative remarks in support of this conclusion. One can see the following from the data (Fig. 4): (1) the $\nu=1$ effect is substantially stronger in Ref. 26 than in Ref. 25; (2) the data of Ref. 26 show both $\nu=1$ and $\nu=3$ QHE while in Ref. 25 $\nu=3$ is absent; and (3) the estimated value of $\Delta_{sas}\approx 13$ K (Ref. 26), 3 K (Ref. 25) is substantially larger in Ref. 26 than in Ref. 25. The conclusion from these qualitative considerations is that the nature of the $\nu=1$ QHE in Refs. 25 and 26 is qualitatively different: In Ref. 25, the incompressible 111 state, stabilized by a many-body gap created by interwell Coulomb correlation, is observed whereas in Ref. 26, the single-particle $\nu=1$ QHE, stabilized by the Δ_{sas} gap created by interwell tunneling, is seen. (This is in sharp contrast to our earlier assertion that the nature of the $\nu=\frac{1}{2}$ FQH states in the two experiments is the same, namely, the 331 many-body state which is robust in the presence of some interwell tunneling.) Later in this article, we present our calculated phase diagram for the transition between these two $\nu=1$ ground states in the $\Delta_{sas}-d/l_c$ space. Our phase diagram, based on the exact diagonalization of small systems, is qualitatively different (i.e., has a different topology) from earlier published results[30] using a single-mode approximation.

The rest of this article is organized as follows. In Sec. II we describe our theoretical calculations. In Sec. III we present and discuss our numerical results (mostly for the $\nu=\frac{1}{2}$ case, some results for the $\nu=1$ and $\frac{2}{3}$ cases as well). We conclude in Sec. IV with a discussion.

II. THEORY

Our technique for studying the FQHE in DQW structures is the exact finite-size diagonalization[32,33] of few electron spherical systems. This extensively used numerical technique has been very successful in the theoretical studies of many different aspects of FQHE. A particularly appealing aspect of the finite-size diagonalization calculation, that we will exploit in this paper, is that by calculating the overlap between the exact numerical (few-electron) many-body wave function and a proposed (or guessed) analytical many-body wave function, one can make a reasonable inference about the nature of the incompressible ground state. (In fact, this technique has been instrumental[32] in establishing the quantitative validity of Laughlin's wave function for the FQHE problem.)

All our calculations are for the "balanced"[25,26] situation where the average electron density ($N/2$) in each well is equal. The generalized N-electron Jastrow-type incompressible Laughlin wave function for the DQW system[4] can then be writtin as (in the planar geometry)

$$\Phi_{m,m,n}(u_1,\ldots,u_{N/2};w_1,\ldots,w_{N/2}) = \prod_{1\le i<j\le N/2}(u_i-u_j)^m \prod_{1\le i'<j'\le N/2}(w_{i'}-w_{j'})^m \prod_{\substack{1\le i''\le N/2\\ 1\le j''\le N/2}}(u_{i''}-w_{j''})^n \times\exp\left\{-\sum_{i=1}^{N/2}|u_i|^2/4l_c^2-\sum_{i'\le 1}^{N/2}|w_{i'}|^2/4l_c^2\right\}, \tag{2}$$

where $u_i=x_i-iy_i$ and, $w_{i'}=x_{i'}-iy_{i'}$ denote the complex 2D coordinate of an electron in the two wells, respectively. The total 2D wave function is obtained by properly antisymmetrizing the orbital part given by Eq. (2),

$$\Psi_{mmn}=\hat{\mathcal{A}}\{\Phi_{m,m,n}(u_1,\ldots,u_{N/2};w_1,\ldots,w_{N/2}) \times l_{u_1}\cdots l_{u_{N/2}}r_{w_1}\cdots r_{w_{N/2}}\}, \tag{3}$$

where l_u and r_w are the pseudospin parts (i.e., the well index) of the wave function for the left and the right wells, respectively, and $\hat{\mathcal{A}}$ is the antisymmetrization operator. The exponents m and n appearing in Eq. (2) are integers which describe the intrawell and interwell Coulomb correlations, respectively (i.e., the interaction between the same and different pseudospins). It is clear that this variational Jastrow wave function, which we will equivalently refer to as the mmn state or the Ψ_{mmn} state, has many-body correlations, similar to that in the original Laughlin wave function, built into it in the multicomponent context. It is also obvious that this DQW incompressible wave function is strictly valid only in the limit of vanishing interwell tunneling (i.e., $\Delta_{sas}=0$) because it treats the electrons (with coordinates denoted by u and w) in the two wells (l and r) as distinguishable species, a picture that breaks down with increasing tunneling. But, as emphasized in the Introduction, the crucial physics underlying FQHE is the incompressibility (i.e., the existence of a gap in the excitation spectra) induced by short-range electron correlations, and, therefore, ground-state wave functions such as the one defined by Eqs. (2) and (3) are quite robust and can be a very good variational ground state even in the presence of some interwell tunneling. The two-component wave function, defined by Eqs. (2) and (3), was first written down[4] by Halperin in the context of the spin generalization of Laughlin's wave function. The applicability of such wave functions to the DQW problem, with the interpretation of the layer index as a pseudospin, was first noted in Ref. 16.

It is obvious that the Pauli principle or Fermi statistics restricts m to be an odd integer. On the other hand, the electrons in the two wells being distinguishable, n can be odd, even, or zero (it cannot be a fraction for reasons of analyticity). The wave function Ψ_{mmn}, just as the Laughlin wave function, is explicitly constructed to be entirely in the lowest Landau level and it is easy to show that it corresponds to a total filling factor given by

$$\nu=\frac{2}{(m+n)}. \tag{4}$$

The wave function also has the property that the electrons with the same pseudospin have relative angular momenta at least m, and those with opposite pseudospin have relative angular momenta at least n. Note also that the wave function, by construction, is an eigenstate of the "z component" of the pseudospin (by taking the two eigenstates of the z component of the pseudospin to represent electrons localized in the left and the right wells, respectively), but *not*, in general, that of the total pseudospin except for the special situations $m=n+1$ or n. Thus, only for these special values of m and n (i.e., $m=n$ or $m=n+1$) can this state be considered to be a good candidate for a pseudospin-conserving interaction Hamiltonian because only under those conditions does the wave function defined by Eqs. (2) and (3) obey the Fock cyclic condition. This makes it problematic[10,11] to use such wave functions in the problem of (real) spin-induced anomalies[12] around $\nu=\frac{1}{2}$ (in the single-layer problem) because the Coulomb interaction being spin independent, the ground-state wave function must be eigenstates of both the total spin and the z component of the spin and, therefore, no good $\nu=\frac{1}{2}$ state can be written down which satisfies Eqs. (2)–(4) and these conditions (i.e., $m=n+1, m=n$). For the DQW problem, however, the Hamiltonian explicitly depends on the pseudospin index because the intrawell and interwell Coulomb interactions are different, and therefore, the DQW states need not be eigenstates of total pseudospin (and we do not need to worry about the Fock condition). Thus, m and n are, respectively, allowed to be any odd integer (m) and any integer or zero (n) in the DQW problem. In particular, the state with $m=3$, $n=1$ (i.e., Ψ_{331}), which we will also refer to as the 331 state, is an allowed state at $\nu=\frac{1}{2}$. Similarly, $m=1$ and $n=1$, corresponding to the 111 state, is an allowed state at $\nu=1$, and, $m=3$, $n=0$, corresponding to the 330 state, is allowed at $\nu=\frac{2}{3}$. These are the three analytic states of the type defined by Eqs. (2)–(4) we consider and compare with our numerical wave functions in this paper.

The many-body Hamiltonian employed in our finite-size diagonalization studies can be written in the second quantized representation as

$$H=\frac{\Delta_{sas}}{2}\sum_m(c^\dagger_{ma}c_{ma}-c^\dagger_{ms}c_{ms}) +\tfrac{1}{2}\sum_{\substack{m_1\alpha_1m_2\alpha_2\\ m'_1\alpha'_1m'_2\alpha'_2}}\langle m'_1\alpha'_1m'_2\alpha'_2|U|m_1\alpha_1m_2\alpha_2\rangle \times c^\dagger_{m'_1\alpha'_1}c^\dagger_{m'_2\alpha'_2}c_{m_2\alpha_2}c_{m_1\alpha_1}, \tag{5}$$

where $c^\dagger_{m\alpha}$ ($c_{m\alpha}$) is the creation (destruction) operator for an electron in the single-electron state $|m\alpha\rangle$ where m is the orbital angular momentum specifying the single-particle wave function on the sphere and α ($\equiv s,a$) denotes the symmetric and the antisymmetric states (with

Δ_{sas} the tunneling-induced symmetric-antisymmetric single-particle gap) associated with the z motion of the two wells. Putting $\Delta_{sas}=0$ will give us the model Hamiltonian considered earlier in Refs. 21 and 22 (where additional approximations were made on the interaction term as well). The electron-electron interaction U in Eq. (5) is the spherical representation of the Coulomb interaction $V_c(\mathbf{r}_1,\mathbf{r}_2)$ [with $\mathbf{r}\equiv(\mathbf{R},z)$, as the three-dimensional electron coordinate vector],

$$V_c(\mathbf{r}_1,\mathbf{r}_2)=\frac{e^2}{\varepsilon[(\mathbf{R}_1-\mathbf{R}_2)^2+(z_1-z_2)^2]^{1/2}} . \tag{6}$$

The spherical representation U for the electron-electron interaction is given by

$$U\equiv\frac{e^2}{\varepsilon[R^2(\hat{\Omega}_1-\hat{\Omega}_2)^2+(z_1-z_2)^2]^{1/2}} , \tag{7}$$

where R is the radius of the sphere and $\hat{\Omega}_{1,2}$ are unit vectors on the sphere defining the positions of the two electrons. The spherical electron-electron interaction U becomes the planar Coulomb interaction V_c for the infinite system.

The single-electron states $|m\alpha\rangle$ are obtained by solving Schrödinger's equation for our model potential (Fig. 1) defined in the Introduction. Since we use a finite spherical geometry to describe the electron motion in the 2D x-y plane, the single-particle eigenstates $|m\alpha\rangle$ in the lowest Landau-level approximation can be written as

$$\langle\mathbf{r}|m\alpha\rangle\equiv\phi_{m\alpha}(\hat{\Omega},z)=f_\alpha(z)Y_{S,S,m}(\hat{\Omega}) , \tag{8}$$

where $Y_{S,S,m}(\hat{\Omega})$ is the monopole spherical harmonic with $-S\le m\le S$ (with $2S=0,1,2,\ldots$, as the number of quantum fluxes through the surface of the sphere), and $f_\alpha(z)$, the eigenfunction for the z part of the single-electron Hamiltonian, satisfies the equation

$$-\frac{\omega_c}{2}\frac{d^2f_\alpha(z)}{dz^2}+V(z)f_\alpha(z)=E_\alpha f_\alpha(z) , \tag{9}$$

where we use l_c and $e^2/\varepsilon l_c$ as the length and energy units, respectively, and ω_c is the Landau-level spacing in this energy unit. The potential $V(z)$ is that defined by Fig. 1,

$$V(z)=\begin{cases} V_w , & |z|\ge b \\ V_b , & |z|\le a \\ 0 , & a\le|z|\le b , \end{cases} \tag{10}$$

where the lengths a and b are related to the barrier thickness D_b and the well width D_w depicted in Fig. 1,

$$a=D_b/2 ; \quad b=\frac{D_b}{2}+D_w . \tag{11}$$

In order for the confinement potential $V(z)$ given in Eq. (10) to describe a real DQW, the eigenequation, Eq. (9), must have at least two bound-state solutions corresponding to the symmetric ($\alpha\equiv s$) and the antisymmetric ($\alpha\equiv a$) states, with $\Delta_{sas}=E_a-E_s$ as the energy difference between them. In any case, we are interested in the two lowest bound solutions ($\alpha=s$ and a) of Eq. (9).

The symmetric bound state is given by

$$f_s(x)=\begin{cases} A_s\cosh(p_sz) , & |z|\le a \\ B_s\sin(k_sz)+C_s\cos(k_sz) , & a\le|z|\le b \\ D_s\exp(-q_s|z|) , & |z|\ge b , \end{cases} \tag{12}$$

where A_s, B_s, C_s, and D_s are constants to be determined by boundary conditions and normalization. The parameters k_s, p_s, and q_s are related to the eigenenergy E_b by

$$k_s^2=\frac{2E_s}{\omega_c} , \tag{13}$$

$$p_s^2=\frac{2}{\omega_c}(V_b-E_s) , \tag{14}$$

$$q_s^2=\frac{2}{\omega_c}(V_w-E_s) , \tag{15}$$

Using boundary conditions on the wave function f_s, we obtain the following eigenvalue problem for the above parameters:

$$[p_s\tanh(p_sa)\sin(k_sa)-k_s\cos(k_sa)][q_s\cos(k_sb)-k_s\sin(k_sb)]=[p_s\tanh(p_sa)\cos(k_sa)+k_s\sin(k_sa)]\times[k_s\cos(k_sb)+q_s\sin(k_sb)] . \tag{16}$$

The eigenvalue problem defined by Eq. (16) can be solved by iteration.

Similarly, the antisymmetric bound-state wave function $f_a(z)$ is given by

$$f_s(z)=\begin{cases} \mathrm{sgn}(z)A_a\cosh(p_az) , & |z|\le a \\ \mathrm{sgn}(z)[B_a\sin(k_az)+C_a\cos(k_az)] , & a\le|z|\le b \\ \mathrm{sgn}(z)D_a\exp(-q_a|z|) , & |z|\ge b . \end{cases} \tag{17}$$

The parameters k_a, p_a, and q_a are given by

$$k_a^2=\frac{2E_a}{\omega_c} , \tag{18}$$

$$p_a^2=\frac{2}{\omega_c}|V_b-E_a| , \tag{19}$$

$$q_a^2=\frac{2}{\omega_c}|V_w-E_a| \ . \tag{20}$$

The eigenvalue equation for the antisymmetric state, also to be solved by iteration, is

$$[p_a\coth(p_a a)\sin(k_a a)+k_a\cos(k_a a)][q_a\cos(k_a b)-k_a\sin(k_a b)]=[p_a\coth(p_a a)\cos(k_a a)-k_a\sin(k_a a)] \times[k_a\cos(k_a b)+q_a\sin(k_a b)] \ . \tag{21}$$

The symmetric-antisymmetric gap entering the Hamiltonian of Eq. (5), $\Delta_{\rm sas}\equiv E_a-E_s=(\omega_c/2)(k_a^2-k_s^2)$, is the energy difference between these lowest symmetric and antisymmetric states for the z motion in the DQW. Because the single-particle states $|m\alpha\rangle$ are known, the matrix elements $\langle m_1'\alpha_1' m_2'\alpha_2'|U|m_1\alpha_1 m_2\alpha_2\rangle$ can be explicitly calculated using the spherical representation, Eq. (7), which in the reduced energy variables becomes

$$U\equiv U(\hat{\Omega}_1,z_1;\hat{\Omega}_2,z_2) =\frac{1}{[S\{(\hat{\Omega}_1-\hat{\Omega}_2)^2+(z_1-z_2)^2\}]^{1/2}} \ . \tag{22}$$

The many-body Hamiltonian of Eq. (5), being completely defined in this manner, can be used to carry out exact finite-size diagonalization of small systems ($N=6-10$ electrons) on the sphere within the lowest Landau level and the lowest symmetric-antisymmetric bound-state approximation as outlined above. To compare the analytical wave functions defined by Eqs. (2)–(4) with our numerical wave functions, we need to transform the proposed planar Jastrow-type many-body wave functions of Eq. (3) to the spherical geometry, which we do using the standard stereographic mapping technique.[33]

Before presenting our numerical results in the next section, we make several remarks regarding the calculation. Our single-electron wave function of Eq. (8) can be written in terms of the "well wave function" g_l and g_r (with l,r denoting the left and the right well, respectively) where,

$$g_l=(f_s+f_a)/\sqrt{2} \ , \qquad g_r=(f_s-f_a)/\sqrt{2} \ . \tag{23}$$

When the two quantum wells are very well separated, the well index (l,r) becomes a good quantum number and the single-particle eigenstates are extremely well approximated by the quantum-well wave function

$$\phi_{m\alpha}\equiv g_\alpha Y_{S,S,m} \ , \tag{24}$$

where $\alpha=l,r$ denotes the well index. Note that, in principle, one can consider $\alpha\equiv(s,a)$ or (l,r) as equivalent sets of pseudospin indices. In the presence of finite interwell tunneling ($\Delta_{\rm sas}\neq 0$), the correct pseudospin label is obviously (s,a), but for weak tunneling [where the mmn-type many-body states defined in Eqs. (2)–(4) are strictly valid], the well index also serves as a good pseudospin index. Our second remark is regarding the interaction matrix elements $\langle m_1'\alpha_1' m_2'\alpha_2'|U|m_1\alpha_1 m_2\alpha_2\rangle$. From symmetry arguments, it is obvious that

$$\langle m_1'\alpha_1' m_2'\alpha_2'|U|m_1\alpha_1 m_2\alpha_2\rangle=0 \quad \text{unless } m_1'+m_2'=m_1+m_2 \ . \tag{25}$$

One last remark is that in all earlier DQW calculations,[21,22,30,31] the overlap between envelope functions centered at different wells was neglected in the calculation of the matrix elements of U. In fact, in all of these earlier calculations, either one explicitly assumed[21,22] $\Delta_{\rm sas}\equiv 0$ [and approximated $f_\alpha(z)$ as δ functions centered at each well], or parametrized[31] $\Delta_{\rm sas}$ as a model input variable, still neglecting wave-function overlap between the two wells. In addiiton, the existing $\nu=1$ DQW calculations[30] for $\Delta_{\rm sas}\neq 0$ employ the single-mode approximation in contrast to our exact numerical calculations.

Before concluding this section, we provide[23] the formulas that one obtains for the simplified double-δ-potential model of the DQW system. (We use this simpler model for some of the $\nu=1$ calculations discussed later in this paper.) The double-δ-potential model for the DQW structure can be written as

$$V(z)=-V_0\left[\delta\left[z+\frac{d}{2}\right]+\delta\left[z-\frac{d}{2}\right]\right] \ , \tag{26}$$

where $V_0>0$ is the strength of the δ-function confinement potential and d is the interwell separation. The Schrödinger equation for $f(z)$ as given in Eq. (9) can be easily solved for this confinement, obtaining (in reduced units with $l_c, e^2/\varepsilon l_c$ as units of length and energy, respectively) for the ground state the following symmetric even-parity state:

$$f_s(z)=\begin{cases} A_s\cosh(k_s z) \ , & |z|\le d/2 \\ B_s\exp(-k_s|z|) \ , & |z|\ge d/2 \ . \end{cases} \tag{27}$$

The eigenenergy is

$$E_s=-\omega_c k_s^2/2 \ , \tag{28}$$

where k_s is given by the equation

$$\tanh(k_s d/2)=2V_0/k_s\omega_c-1 \ . \tag{29}$$

The first excited state is the antisymmetric state, which has the odd-parity wave function

$$f_a(z)=\begin{cases} A_a\cosh(k_a z) \ , & |z|\le d/2 \\ \mathrm{sgn}(z)B_a\exp(-k_a|z|) \ , & |z|\ge d/2 \ , \end{cases} \tag{30}$$

where k_a is given by the equation

$$\coth(k_a d/2)=2V_0/k_a\omega_c-1 \ . \tag{31}$$

The eigenenergy for the antisymmetric state E_a for this

double-δ-potential model is given by

$$E_a = -\omega_c k_a^2/2 \ . \tag{32}$$

Note that one must have $V_0 d/\omega_c > 1$ for there to be at least two bound states (the s and a states) in this model.

The coefficients $A_s(A_a)$ and $B_s(B_a)$ in the above equations are determined, as usual, by boundary conditions and normalization. The symmetric-antisymmetric gap

$$\Delta_{\rm sas} = |E_a - E_s| = \frac{\omega_c}{2}(k_a^2 - k_s^2)$$

can be determined for this model from Eqs. (27)–(32) which are just the simplified double-δ-potential model versions of the more general Eqs. (12)–(21) which are valid for the realistic DQW model. Note that the double-δ-potential model is totally defined by the two parameters d and V_0, whereas the realistic DQW model has, in general, four parameters, V_w, V_b, D_w, D_b. Note that for the δ-potential model, one can equivalently consider d and $\Delta_{\rm sas}$ as the independent input parameters (instead of d and V_0) characterizing interwell Coulomb interaction and interwell tunneling, respectively. (This, in fact, is the model we use for calculating our $\nu=1$ phase diagram.) Note that the δ charge-density model,[21,22] the simplest model for DQW structures, is characterized by *only* one parameter, namely, d.

In the next section we present our numerical results and discuss them (for $\nu=\frac{1}{2}$) in light of the recent experiment results in DQW systems.[25,26] We use the actual experimental well parameters corresponding to Refs. 25 and 26 as shown in Figs. 2 and 3, respectively, for our $\nu=\frac{1}{2}$ DQW calculations. Our $\nu=1$ and $\frac{2}{3}$ calculations are done for experimentally accessible model parameters, but the emphasis is more on qualitative aspects. We present the excitation spectra based on our direct diagonalization (for $N=6$–10 electron spherical systems) calculations. We also calculate the overlap between our numerical finite-system ground-state wave function and various (proposed) analytical wave functions of the *mmn* type [Eqs. (2)–(4)] to investigate the nature of our incompressible state, and, if possible, to map out the phase diagram (as a function of system parameters) for fixed values of ν.

III. RESULTS

We present our numerical results in subsections A–D, dealing, respectively, with $\nu=\frac{1}{2}$ FQHE for the AT&T experiment of Ref. 25, $\nu=\frac{1}{2}$ FQHE for the Princeton experiment of Ref. 26, the $\nu=1$ situation using model parameters, and the $\nu=\frac{2}{3}$ situation using model parameters. In the first two subsections, we use the actual sample parameters used in the experiments of Refs. 25 and 26 as given in our Figs. 2 and 3, respectively. Our results, therefore, can be compared directly with the experimental data. We use the GaAs effective mass and lattice dielectric constant in our numerical calculations—our dimensionless energy is expressed in units of $e^2/\varepsilon l_c$ and dimensionless length in units of l_c. The presented results, unless otherwise stated, are for $N=6$ electron systems.

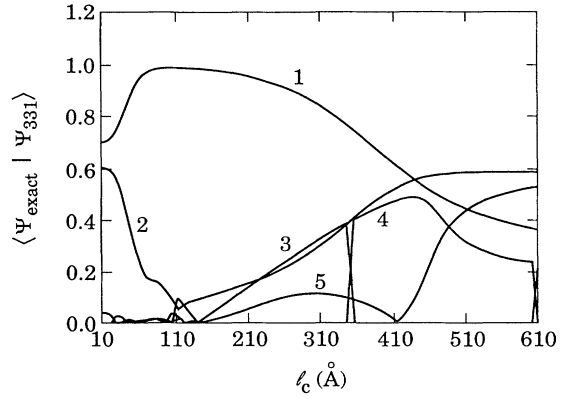

FIG. 5. Calculated overlap between the proposed wave function Ψ_{331} and the first few lowest-energy exact finite-system numerical states as a function of the magnetic length l_c for the AT&T sample (Ref. 25). The sample parameters of the double quantum well (Ref. 25) used in the calculation (Fig. 2) are the following: $D_w=120$ Å, $D_b=51$ Å, $V_w=V_b=750$ meV. This gives $\Delta_{\rm sas}=0.14$ meV. (1–5 in the figure correspond to the ground state up to the fourth excited many-body state, respectively.) In Ref. 25, $\nu=\frac{1}{2}$ FQHE is observed for $l_c\sim 90$ Å where the overlap is large.

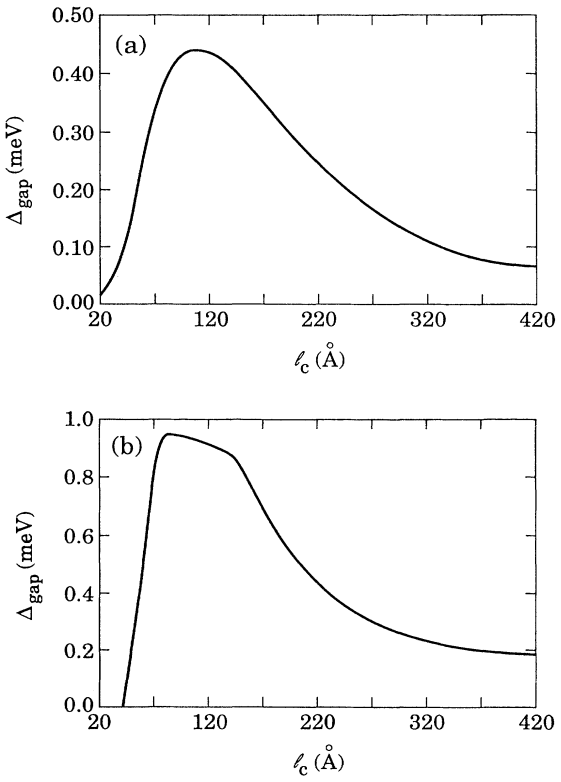

FIG. 6. (a) The calculated roton gap as a function of the magnetic length l_c in the sample specified in Fig. 5. (b) The calculated excitation gap for creating a well-separated quasiparticle-quasihole pair as a function of the magnetic length l_c in the sample specified in Fig. 5.

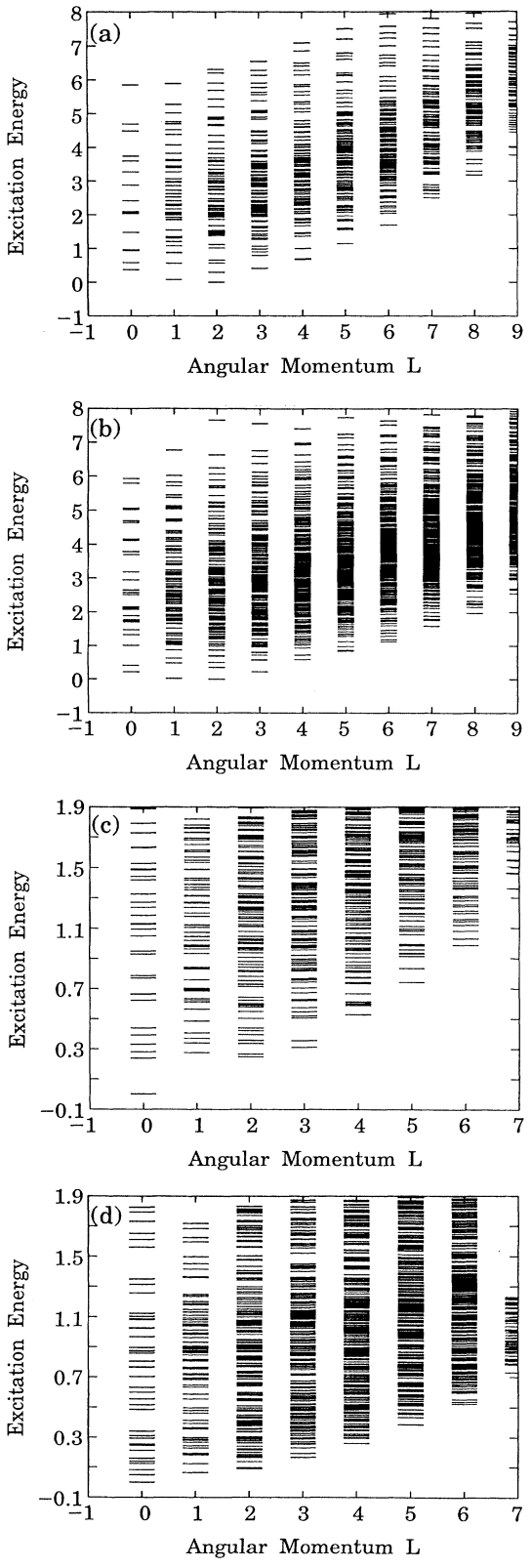

FIG. 7. Calculated excitation spectra for the sample specified in Fig. 5 as a function of the total angular-momentum quantum number L. Energy is measured in units of $e^2/\varepsilon l_c$. The calculations are for (a) $l_c = 30$ Å, (b) 100 Å, (c) 220 Å, and (d) 420 Å.

A. $\nu = \frac{1}{2}$ FQHE in the AT&T samples (Fig. 2)

The sample parameters, as given in Fig. 2, are $V_b = V_w = 750$ meV, $D_w = 120$ or 180 Å, and $D_b = 51$, 31, or 99 Å (depending on the situation). This leads to a $\Delta_{sas} \sim 0.1$ meV for the AT&T samples. In Figs. 5–9, we show our numerical exact diagonalization results for a few different AT&T samples, all of which are characterized by a high and narrow barrier ($V_w = V_b = 750$ meV) separating the two wells. In Figs. 5–8 we use $D_w = 120$ Å, $D_b = 51$ Å while in Fig. 9, $D_w = 180$ Å and $D_b = 31$ and 91 Å.

In Fig. 5, we plot the calculated overlap of the exact numerical wave function with the 331 state as a function of the magnetic length l_c for a fixed set of sample parameters ($D_w = 120$ Å, $D_b = 51$ Å). We show the overlap between the proposed Ψ_{331} wave function with the five lowest-energy states of our numerical calculation. As one can see for $l_c \approx 50$–300 Å, the overlap between Ψ_{331} and the numerical exact ground state is large (almost unity), indicating that the system is very well approximated by the 331 incompressible state exhibiting $\nu = \frac{1}{2}$ FQHE in this parameter range. Note two significant features of the results depicted in Fig. 5, which seem to be general characteristics of all the DQW incompressible states investigated by us. One feature is that the 331 state remains a reasonable approximation to the exact numerical state (i.e., the overlap is large) *over a range of values of*

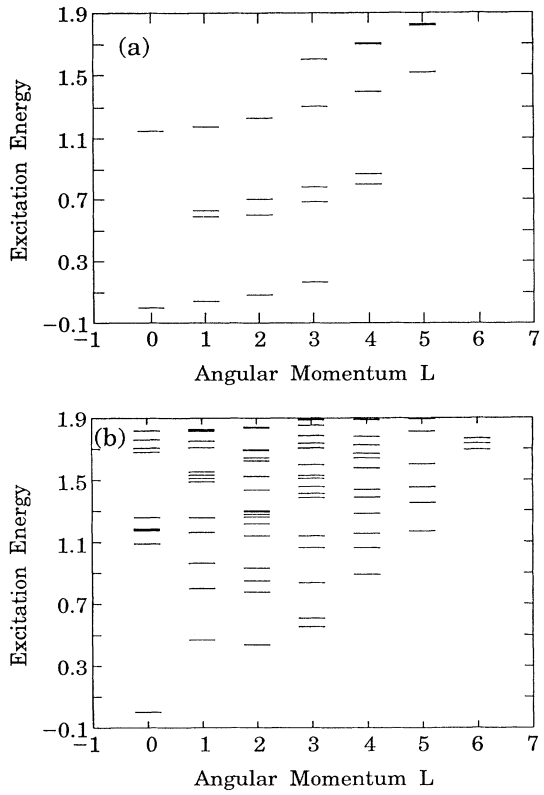

FIG. 8. (a) Calculated excitation spectra for the same sample as in Figs. 5–7 with two additional quasiparticles ($l_c = 100$ Å). (b) Same as in (a) with two additional quasiholes.

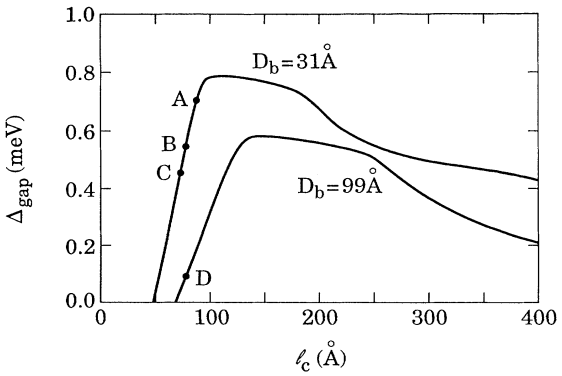

FIG. 9. Calculated quasiparticle-quasihole excitation gap as a function of the magnetic length l_c for the samples (A, B, C, and D) used in the experiment of Eisenstein *et al.* (Ref. 25). The sample parameters (Fig. 2) are the following: well width $D_w = 180$ Å, barrier height and well depth $V_b = V_w = 750$ meV. The samples are different in their barrier thicknesses as indicated in the figure. The experimentally measured approximate gaps are also shown. (The experimental points should be taken to imply the strength of the gap, rather than an absolute measurement.)

l_c—this is a general feature of incompressibility, once the condition for incompressibility is satisfied, it remains valid over a range of values of the system parameters (explaining why, as we will see later, the 331 state is robust even in the presence of finite values of Δ_{sas}). The second noteworthy feature is that the region of Fig. 5 where the overlap of the numerical *ground* state with the 331 state is high (for $l_c \sim 50-300$ Å) is roughly the same region where the overlap of the 331 state with the numerical *excited* states is small and vice versa, as it should be if the 331 state is the correct ground state for the system. We point out that experimentally,[25] the strongest $\nu = \frac{1}{2}$ FQHE is observed around $l_c \approx 90$ Å which is roughly where the overlap of the exact ground-state wave function with the 331 state is the maximum in Fig. 5, indicating clearly that the 331 state is being observed in Ref. 25.

In Fig. 6(a), we show, as a function of l_c, our calculated "optical" excitation gap at the roton minimum[34] (i.e., the roton gap) which is the minimum energy required to produce a neutral collective excitation in the $\nu = \frac{1}{2}$ state of the sample of Fig. 5. The numerically calculated gap is appreciable only in the region where 331 is a good approximation to the ground state of the system, reinforcing again the fact that the system is an incompressible $\nu = \frac{1}{2}$ state only in the region $l_c \sim 50-300$ Å. In Fig. 6(b), we show the calculated transport excitation gap needed to produce well-separated quasiparticle-quasihole pairs—this is presumably the gap measured as the activation energy in transport experiments. The calculated activation gap is of the order of 1 meV, quite comparable to the strength of the very best primary single-layer odd-denominator FQH states (i.e., the $\nu = \frac{1}{3}$ FQHE). The activation gap, as one expects, is appreciable only for a range of values of l_c where the system is in the incompressible 331 $\nu = \frac{1}{2}$ FQH state.

In Fig. 7, we show our calculated excitation spectra as a function of the total angular-momentum quantum number L for (a) $l_c = 30$ Å, (b) 100 Å, (c) 220 Å, and (d) 420 Å (and for the same sample as in Figs. 5 and 6). Note that our units are reduced units with energy expressed in $e^2/\varepsilon l_c$ and length in l_c.

In Figs. 8(a) and 8(b), we depict the calculated excitation spectra (for the same sample) in the presence of two additional quasielectrons and two additional quasiholes, respectively.

Finally, in Fig. 9, we provide a direct comparison of our numerical results with the experimental data[25,35] of Eisenstein *et al.* by showing the measured excitation energies (obtained via the usual activated transport studies) at the $\nu = \frac{1}{2}$ FQHE on our theoretical plots for four different samples with two different barrier thicknesses of 31 Å (data points A, B, C corresponding to samples with three different carrier densities) and 99 Å (data point D), respectively. The agreement between theory and experiment[25,35] is particularly remarkable because the theory contains no adjustable parameters and used the materials parameters of the experimental DQW sample. We believe that such an excellent agreement between theory and experiment shows unambiguously that the theory of FQHE in DQW structures (and, by implication, the multicomponent generalization of the Laughlin theory as carried out in this paper) is quantitatively and qualitatively accurate.

These results (Figs. 5–9) establish that the $\nu = \frac{1}{2}$ FQHE observed[25] in the DQW structures by the AT&T group is the 331 multicomponent generalized Laughlin-type incompressible ground state. Not only was the $\nu = \frac{1}{2}$ FQHE in the DQW system predicted[23,24] by the theory, the theoretical results are in excellent quantitative agreement with experiment without adjusting any parameters.

B. $\nu = \frac{1}{2}$ FQHE in the Princeton samples (Fig. 3)

As discussed in Sec. I, the Princeton sample[26] (Fig. 3) is actually a wide single quantum well where the self-consistent electric field created by the electrons produces an effective DQW system with the electrons accumulating near the two edges of the well with the charge density showing a double-humped structure. The model parameters for this effective DQW system used in our FQHE calculations can easily be obtained from a self-consistent calculation and one gets the following[26] (Fig. 3): $D_w = 220$ Å, $D_b = 120$ Å, $V_w = 1.2$ eV, and $V_b = 25$ meV, which are substantially different from those used[25] for the AT&T samples. (As mentioned in Fig. 2, our parameters are somewhat different from those in Ref. 26—our neglect of self-consistency effects in the z part of Schrödinger's equation, Eq. (9), demands that we use modified values of the DQW parameters to reproduce the correct self-consistent charge density and the Δ_{sas} value of Ref. 26.) The main qualitative difference between the two samples is a substantially lower (but somewhat wider) potential barrier V_w separating the two electron layers in the Princeton sample[26] compared with the AT&T samples. This leads to enhanced interwell tunneling in the Princeton sample, producing a rather large symmetric-antisymmetric gap of $\Delta_{sas} \sim 1$ meV (compared with

$\Delta_{sas} \sim 0.1$ meV for the AT&T samples). We show, in Figs. 10–12, that the 331 incompressible state survives this level of interwell tunneling, and the $\nu = \frac{1}{2}$ FQHE observed in Ref. 26 is qualitatively the same 331 ground state seen in Ref. 25. As emphasized before, short-range correlation-induced Laughlin-type incompressible states are often robust and can usually survive (up to some extent) physical mechanisms which oppose incompressibility.

In Fig. 10, we show, as a function of l_c, our calculated overlap between the exact numerical ground state and the 331 state for the Princeton sample. The overlap is qualitatively similar to that (Fig. 5) for the AT&T sample except that the range of the magnetic length ($l_c \sim 50-100$ Å) where the overlap is large (i.e., close to unity) is substantially smaller than that ($l_c \sim 50-300$ Å) for the AT&T sample. We therefore conclude that the Princeton sample should exhibit a $\nu = \frac{1}{2}$ FQHE corresponding to the 331 state in a narrow range of magnetic field values around $l_c \approx 50-100$ Å and, in fact, in Ref. 26 the $\nu = \frac{1}{2}$ FQHE shows up for $l_c \sim 70$ Å ($B = 14-15$ T) which is roughly where our calculated overlap with the 331 state is a maximum in Fig. 10! This excellent agreement obtained without any adjustable parameter makes us confident that the FQH state observed in Ref. 26 is indeed the 331 state, just as it is for the experiment of Ref. 25, in spite of the presence of substantial interwell tunneling in the Princeton sample (which, of course, our numerical calculation includes exactly). This point is further reinforced by the density dependence of the observed effect.[26] Our results (Fig. 11) predict that the $\nu = \frac{1}{2}$ FQHE will become weaker if the electron density is increased, which is precisely the experimental observation.[26] If the pairing mechanism of Ref. 28 is operative, an increase of density should enhance the $\nu = \frac{1}{2}$ FQHE, contrary to the experimental finding.[26]

In Fig. 11 we show, as a function of l_c, our calculated activation gap for the sample of Ref. 26. The experimentally measured activation gap, also shown in Fig. 11, agrees well with our theoretical calculation (again, with no adjustable parameter), showing the quantitative validity of the calculation.

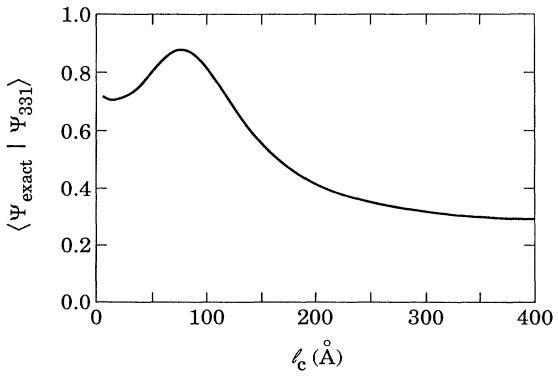

FIG. 10. Calculated overlap between the Ψ_{331} state and the exact numerical ground state as a function of the magnetic length l_c for the Princeton sample (Ref. 26) (Fig. 3). In Ref. 26, $\nu = \frac{1}{2}$ FQHE is observed for $l_c \sim 70$ Å where the overlap is large.

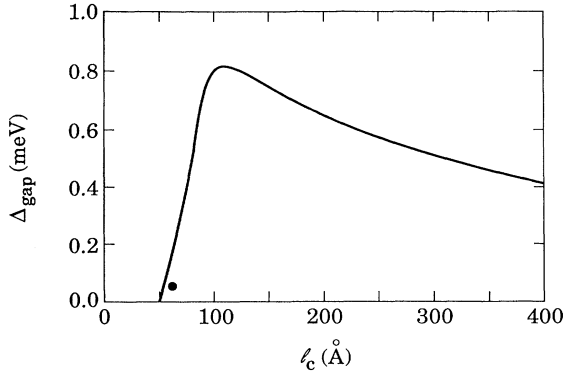

FIG. 11. Calculated excitation gap as a function of the magnetic length l_c for the Princeton sample (Ref. 26) (Fig. 3). The experimentally measured excitation gap is shown in the figure.

In Fig. 12, we show the calculated excitation spectra at $\nu = \frac{1}{2}$ for the sample corresponding to Fig. 3 and for (a) $l_c = 60$ Å, (b) 100 Å, (c) 150 Å, (d) 200 Å, (e) 300 Å, and (f) 400 Å.

The qualitative similarity between the results for the samples of Figs. 2 and 3 shows that the same ground state (viz. the 331 state of Halperin) occurs in both experiments.[25,26] The substantial overlap between the numerical ground state and the 331 state around the experimental magnetic-field values where the $\nu = \frac{1}{2}$ FQHE is observed[25,26] establishes that the observed $\nu = \frac{1}{2}$ FQHE is due to the theoretically predicted 331 incompressible state in both[25,26] experiments. We note that the large bare value of Δ_{sas} in Ref. 26 does not rule out the existence of the 331 state because Coulomb interaction may strongly renormalize Δ_{sas} and the *renormalized* Δ_{sas} is the relevant parameter determining the nature of the DQW ground state. Our numerical results suggest that the renormalized Δ_{sas} in Ref. 26 is small enough for the 331 state to be the ground state.

Finally, we show in Fig. 13 the calculated excitation spectra as a function of the magnetic length in the total angular momentum $L = 0$ sector of the Hilbert space for the experimental samples of Refs. 25 and 26 in the $\nu = \frac{1}{2}$ situation. (The incompressible ground state is expected to belong to the $L = 0$ subspace for our finite spherical system calculation.) For each magnetic length, the spectra have been shifted so that the ground-state energy is always zero, showing the excitation energy as a function of l_c. The level crossing behavior in Fig. 13 provides direct information about the nature of the strongly correlated states and the quantum phase transition between them in the $\nu = \frac{1}{2}$ DQW problem. The structure of the level crossing (and, in particular, anticrossing) depends on the local symmetry of the Hilbert space. If, due to some local symmetry, the Hamiltonian at the would-be crossing point does not couple the two (almost degenerate) states, the crossing will be a direct one and the degeneracy will not be lifted. Otherwise, there will be an anticrossing, signifying a quantum phase transition, if it happens for the ground state, at the value of l_c. In both Figs. 13(a) and 13(b), there are two anticrossings for the

ground state, signifying two quantum phase transitions. It is significant that these anticrossings occur around the same values of l_c ($\sim$80 and 180 Å) in both Refs. 25 and 26. The first anticrossing occurs at around $l_c \approx 80$ Å, indicating a transition from a compressible state to the incompressible 331 state. The second transition, occurring at around $l_c \approx 180$ Å, denotes a transition from the 331 state to another compressible state. The remarkable qualitative similarity of Figs. 13(a) and 13(b) reinforces our earlier assertion that the $\nu = \frac{1}{2}$ FQHE observed in Refs. 25 and 26 belong to the same universality class, namely the 331 state[4] of Halperin. [We point out that our calculated overlap between the exact ground state and the 331 state, as shown, for example, in Figs. 5 and 10, has a substantial overlap (for the sample in Ref. 25 as shown in Fig. 5) for a wider range of $l_c \sim 50$–300 Å, indicating the stability of the 331 state over a wider range of magnetic-field values than that implied by our results ($l_c \sim 80$–180 Å) shown in Fig. 13. This is due to finite-size effects which, for small system sizes ($N = 6$) used in our calculations, keep the overlap large even outside the 331 regime.]

C. $\nu = 1$ QHE in DQW systems

As mentioned in Sec. I, the $\nu = 1$ QHE may arise in DQW structures from two distinct physical mechanisms.

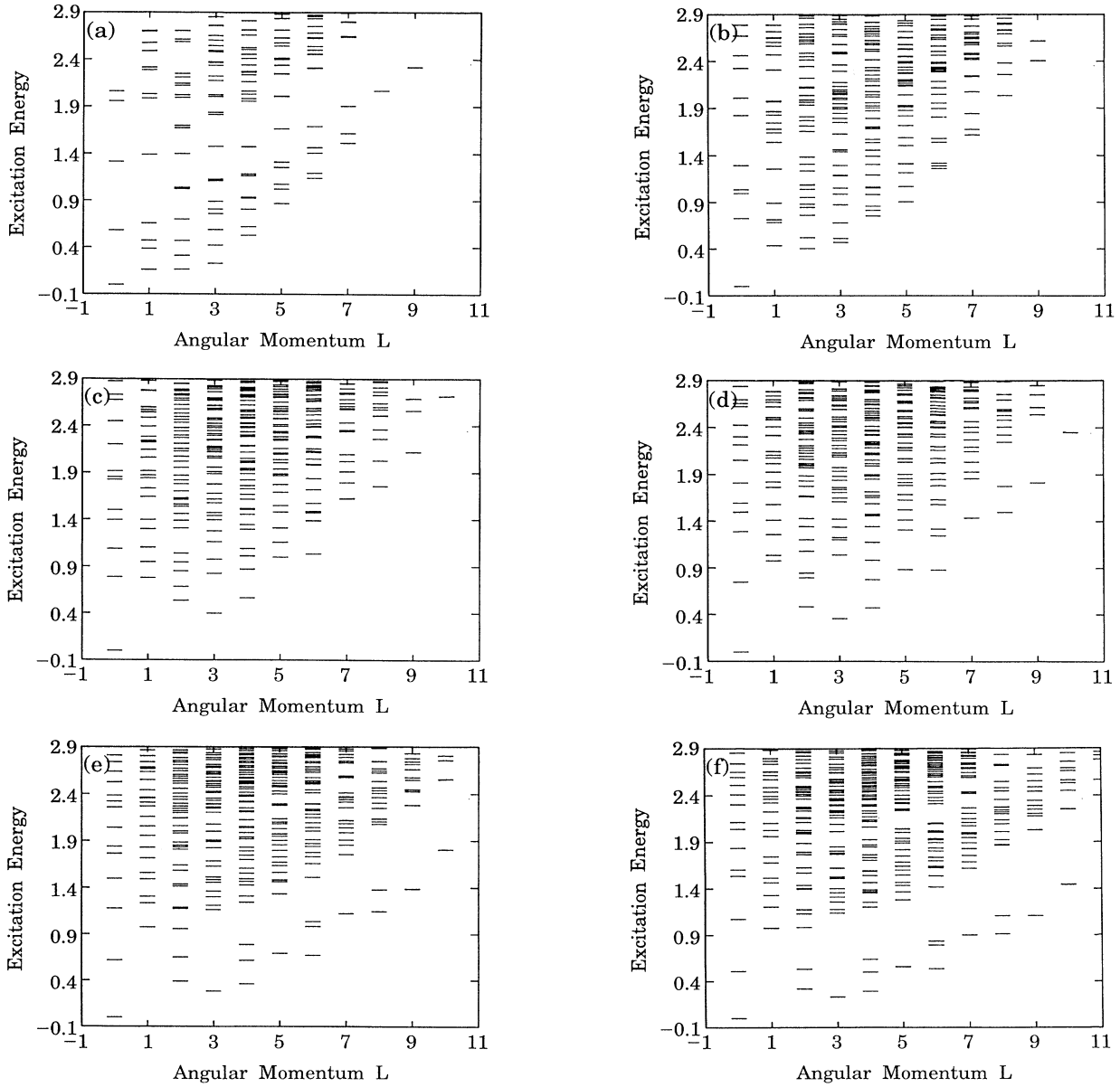

FIG. 12. Calculated excitation spectra as a function of the total angular-momentum quantum number for the Princeton sample (Fig. 2). Energy is measured in units of $e^2/\varepsilon l_c$. Results are shown for (a) $l_c = 60$ Å, (b) 100 Å, (c) 150 Å, (d) 200 Å, (e) 300 Å, and (f) 400 Å.

For the very small interwell separation d, or equivalently, for the large interwell tunneling, the $\nu=1$ QHE is stabilized by the symmetric-antisymmetric gap Δ_{sas}. This is the usual single-particle QHE where electron correlation effects do not play any central role. In this case, the lowest pseudospin state, i.e., the symmetric state s, is totally occupied ($\nu_s=1$) and the antisymmetric state is totally empty (this is formally identical to the usual QHE in single-layer 2D structures in the presence of spin splitting, where the spin-up state is totally occupied and the spin-down state empty at $\nu=1$)—the excitation gap being the single-particle gap Δ_{sas}. We call this Δ_{sas} stabilized (single-particle) incompressible state the $\Psi^{(s)}_{\nu=1}$ state, implying that all the symmetric states (in the lowest Landau level) are occupied. As d increases and Δ_{sas} goes down, this incompressible state is destroyed[29–31] by Coulomb interactions (equivalently, keeping d fixed and increasing the magnetic field also destroys[29] this state because the relative magnitude of Δ_{sas} goes down with respect to the Coulomb correlation energy).

In Figs. 14(a) and 14(b), we show the destruction of the $\nu=1$ QHE in a DQW structure due to increasing (decreasing) d (Δ_{sas}) by depicting the calculated variation of the overlap between our numerical ground state (for $N=8$ electrons) and the $\Psi^{(s)}_{\nu=1}$ incompressible state as a function of d/l_c (and $\Delta_{sas}/[e^2/\varepsilon l_c]$). Note that the overlap remains at unity for $d/l_c \lesssim 1$ and it is essentially zero (of course, it does not quite go to zero because our system is small) for $d/l_c \gtrsim 2$. Thus, the Δ_{sas} stabilized $\nu=1$ QHE is destroyed for $d \lesssim 2l_c$ (and for $\Delta_{sas} \lesssim 0.04e^2/\varepsilon l_c$). Results for Fig. 14(a) are obtained for the double-δ-potential model system as described in Eqs. (26)–(32). In Fig. 14(b) we show our calculated excitation (activation) gap as a function of the magnetic length for a real DQW structure[29] with $D_w=140$ Å, $D_b=40$ Å, $V_w=V_b=250$ meV. One can see that for small magnetic lengths (i.e., a large magnetic field), the $\Psi^{(s)}_{\nu=1}$ incompressible QHE state is

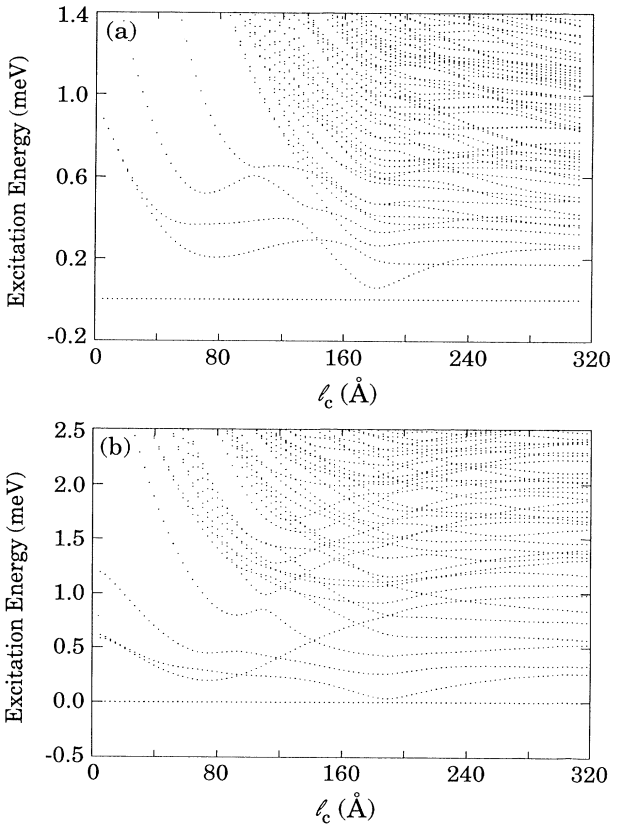

FIG. 13. Calculated excitation spectra (measured with respect to the ground-state energy which is the horizontal line at zero energy) in the zero total angular-momentum sector of the Hilbert space as a function of the magnetic length l_c for the $\nu=\frac{1}{2}$ DQW structure: (a) the sample *A*, *B*, *C* (Fig. 2) of Ref. 25; (b) the sample of Ref. 26 (Fig. 3). The level anticrossing behavior for the ground state around $l_c \sim 80$ Å and 180 Å indicates first-order (quantum) phase transitions from a compressible Fermi liquid state to the 331 incompressible state ($l_c \sim 80$ Å) and then from the 331 state to another compressible liquid state ($l_c \sim 180$ Å).

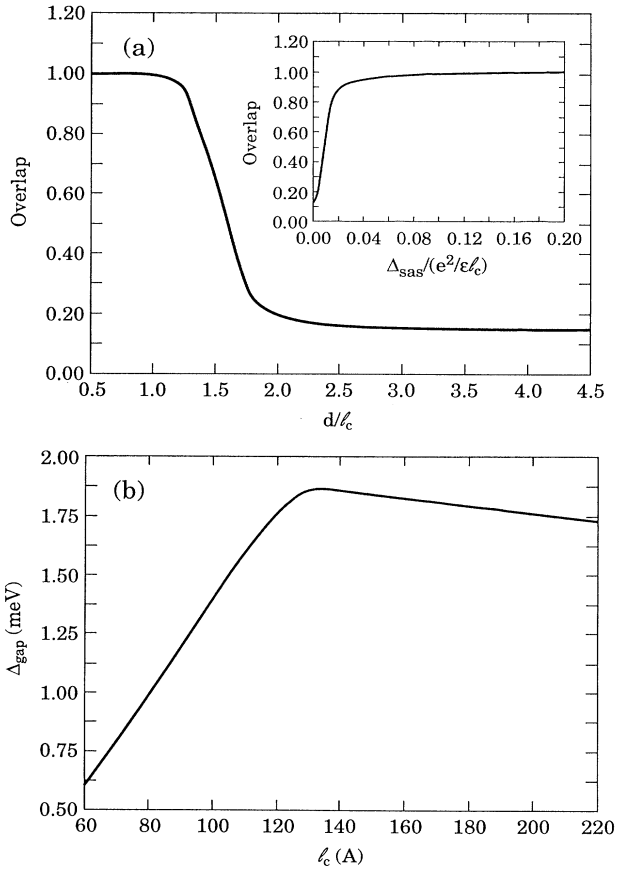

FIG. 14. (a) Calculated overlap between the exact numerical ground state and the $\Psi^{(s)}_{\nu=1}$ state as a function of the well separation d for the $\nu=1$ situation, showing the destruction of incompressibility for large values of d/l_c. The inset shows the overlap as a function of $\Delta_{sas}/(e^2/\varepsilon l_c)$ for fixed $d/l_c=0.50$. (b) Calculated excitation gap as a function of the magnetic length in the $\nu=1$ situation for the well parameters (Fig. 1) $V_w=V_b=250$ meV; $D_w=140$ Å, $D_b=40$ Å. The $\Psi^{(s)}_{\nu=1}$ state is more stable for higher values of l_c.

destroyed. This is the many-body interaction-induced destruction of the QHE investigated experimentally in Ref. 29. Experimentally,[29] the QHE is destroyed around $l_c \sim 100$ Å which compares favorably with our numerical result of Fig. 14(b) where the gap vanishes for $l_c \lesssim 120$ Å.

The physics responsible for the destruction of the $\Psi^{(s)}_{\nu=1}$ QH state in DQW systems is the exponential decrease in Δ_{sas} with increasing well separation d so that eventually electron-electron correlation becomes the dominant energy scale, destroying the individuality of the symmetric and antisymmetric single-particle states (i.e., broadening them). Conversely, decreasing l_c (by increasing the magnetic field) accomplishes the same by making $\Delta_{sas}/(e^2/\varepsilon l_c)$ smaller. The destruction of the $\Psi^{(s)}_{\nu=1}$ state occurs when the renormalized Δ_{sas} vanishes due to Coulomb interaction.

It turns out, however, that, even for $\Delta_{sas}=0$ (which means $\Psi^{(s)}_{\nu=1}$ incompressibility is nonexistent), one may have a many-body $\nu=1$ QHE where the competition between the interwell and intrawell Coulomb correlation produces an incompressible excitation gap. This happens when the correlation effect drives the system into the 111, i.e., the Ψ_{111} many-body ground state which has $\nu=1$ and a many-body excitation gap. Clearly, Ψ_{111} (which is qualitatively similar to the Ψ_{331} state) can be stabilized only at finite values of d/l_c (whereas $\Psi^{(s)}_{\nu=1}$ is stable at small d/l_c). We emphasize that the nature of the Ψ_{111} ground state is qualitatively different from that of the $\Psi^{(s)}_{\nu=1}$ ground state, even though both exhibit $\nu=1$ QHE in DQW structures—the $\nu=1$ effect for the Ψ_{111} state is really a $\nu=1$ FQHE whereas the $\nu=1$ effect for the $\Psi^{(s)}_{\nu=1}$ state is the usual IQHE! Electron-electron interaction destroys the $\Psi^{(s)}_{\nu=1}$ state, and is responsible for stabilizing the Ψ_{111} state.

Since there are two qualitatively different ground states producing the $\nu=1$ QHE in DQW structures, we can try to calculate the phase diagram for the $\nu=1$ filling in a DQW structure in the relevant $d-\Delta_{sas}$ parameter space. We have carried out such an extensive calculation and the result is shown in Fig. 15. We use the simplified double-δ-layer model for this study by considering each well to be a δ layer separted by a distance d and by introducing Δ_{sas} as a parameter (i.e., the four parameters V_w, V_b, D_w, D_b of the realistic DQW model are replaced by two parameters Δ_{sas} and d in the Hamiltonian). The calculation is done by a finite-size diagonalization of an eight-electron system with $\nu=1$. For each value of d and Δ_{sas}, we numerically calculate the overlap of the exact finite-size many-body wave function with the analytical $\Psi^{(s)}_{\nu=1}$ state and with the Ψ_{111} state. If the overlap with a proposed state exceeds 0.9, we consider the system to be in that incompressible state. The result of this exhaustive numerical study is shown as the phase diagram in Fig. 15. The two solid lines represent the boundary of the regions where the overlaps with the $\Psi^{(s)}_{\nu=1}$ and Ψ_{111} states are 0.9. Thus, to the right of the lower 0.9 line, the system is in the $\Psi^{(s)}_{\nu=1}$ incompressible state, exhibiting $\nu=1$ IQHE. This is the region of large tunneling [i.e., "high" values of $\Delta_{sas}/(e^2/\varepsilon l_c)$]. To the left of the upper 0.9 line, the system is in the Ψ_{111} incompressible ground state, exhibiting

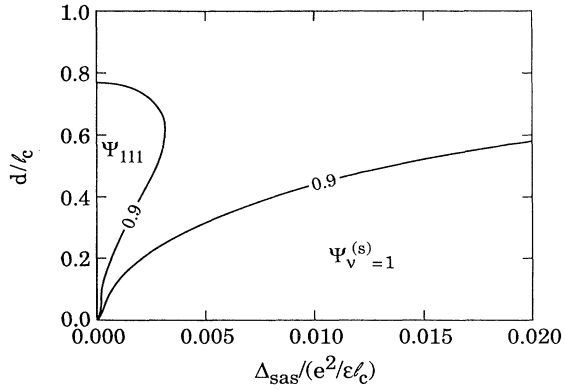

FIG. 15. Calculated phase diagram for the $\nu=1$ QHE in DQW systems as a function of model parameters d/l_c and Δ_{sas} (measured in units of $e^2/\varepsilon l_c$). The solid lines marked 0.9 denote the boundaries of the phases corresponding to incompressible ground states $\Psi^{(s)}_{\nu=1}$ (to the right of the lower line) and Ψ_{111} (to the left of the upper line). The other regions of the phase diagram correspond to compressible liquid states. The solid lines indicate that the calculated overlap of the exact numerical ground state with the $\Psi^{(s)}_{\nu=1}$ (Ψ_{111}) state is higher than 0.9 to the right (left) of the lower (upper) line.

$\nu=1$ FQHE. This is the region of small tunneling. We surmise that there is no other region of QHE in the rest of the phase diagram which is filled with compressible states.

A number of comments about our phase diagram of Fig. 15 are in order. While experiments should be carried out to directly test our pedicted phase diagram, the existing experimental data[25,26,29] in DQW systems qualitatively support our results. The agreement here is only qualitative due to our use of the double-δ-layer model and the neglect of well widths in the calculation of the phase diagram. We also point out that our phase diagram is qualitatively different from that obtained in Ref. 30 by a single-mode approximation. In particular, the $\nu=1$ QHE phase corresponding to the Ψ_{111} state was not considered in Ref. 30. As mentioned in Sec. I, we believe that the $\nu=1$ QHE observed in Ref. 25 corresponds to the Ψ_{111} universality state and that observed in Ref. 26 corresponds to the $\Psi^{(s)}_{\nu=1}$ universality state. This conclusion is consistent with our phase diagram and also with the fact that an in-plane magnetic field, which suppresses Δ_{sas}, has little effect on the $\nu=1$ QHE in Ref. 25 while destroying it in Ref. 26. In Ref. 29, the phase transition between the $\Psi^{(s)}_{\nu=1}$ state and the compressible region was observed by changing the magnetic field {which decreases $\Delta_{sas}/[e^2/(\varepsilon l_c)]$ and increases d/l_c}. Note that the theoretical phase diagram makes a striking prediction of a reentrant $\nu=1$ QHE in a DQW structure either with increasing d at very samll Δ_{sas}, or, with decreasing Δ_{sas} at a fixed value of d. To the best of our knowledge, this reentrant $\nu=1$ QHE in DQW systems has not yet been observed experimentally. We believe that it should be observable in a systematic experimental study.

D. $\nu=\frac{2}{3}$ FQHE in DQW systems

The $\nu=\frac{2}{3}$ FQHE in a DQW structure is qualitatively different from both the $\nu=\frac{1}{2}$ and $\nu=1$ cases studied above because in both the limits of $d=0$ and $d=\infty$, one gets an incompressible many-body state for $\nu=\frac{2}{3}$: At $d=0$, it is the $\Psi^{(s)}_{\nu=2/3}$ state where the symmetric state is totally occupied with $\nu=\frac{2}{3}$ producing the usual $\frac{2}{3}$ FQHE, and, at $d=\infty$, one gets two isolated $\nu=\frac{1}{3}$ single-layer 2D systems with the usual $\frac{1}{3}$ FQHE. The interesting question is what happens in between.

In Fig. 16, we show our calculated overlaps between the exact numerical many-body wave function with the two proposed states, $\Psi^{(s)}_{\nu=2/3}$ and Ψ_{330}, which are expected to be exact for small d and large d, respectively. (Note that the 330 state describes two isolated single 2D layers with $\frac{1}{3}$ occupancy each.) The calculation is carried out for a model system with two δ layers separated by a distance d representing the DQW structure and a fixed value of Δ_{sas} introduced as an input model parameter. One can see that for small separations, the $\Psi^{(s)}_{\nu=2/3}$ state is the ground state, and for large separatins, the Ψ_{330} state is the ground state with a direct transition from one to the other driven by the interwell Coulomb correlation around $d\sim l_c$. We surmise that the $\nu=\frac{2}{3}$ DQW structure *always* exhibits a FQHE (either a $\nu=\frac{2}{3}$ FQHE at small separations corresponding to the $\Psi^{(s)}_{\nu=2/3}$ state, or, two independent $\nu=\frac{1}{3}$ FQHE at large separations corresponding to the Ψ_{330} state) and the phase diagram consists of only two incompressible phases, both exhibiting the same FQHE. There may, however, be a sharp change in the activation energy as one crosses the phase boundary because, once Landau-level coupling, etc., are included, the $\nu=\frac{2}{3}$ and $\frac{1}{3}$ FQHE may have different excitation gaps. An experimental search should be made for the transition shown in Fig. 16.

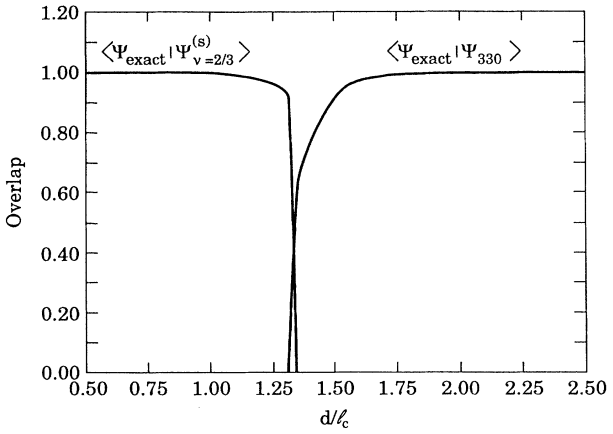

FIG. 16. Calculated overlap of the exact numerical ground state with the $\psi^{(s)}_{\nu=2/3}$ state and the Ψ_{330} state as a function of well separation d/l_c for the $\nu=\frac{2}{3}$ situation.

IV. CONCLUSION

In this paper, we have considered DQW structures in strong external magnetic fields for three different values of the total filling factor $\nu=\frac{1}{2}$, $\frac{2}{3}$, and 1, studying in details the nature of the many-body ground state and the excitation spectra using the finite-size spherical system exact numerical diagonalization technique (in the lowest spin-split Landau level). Using a realistic model of confinement, we have analyzed the role and the interplay of the three relevant energy scales, viz. the intrawell Coulomb interaction, the interwell Coulomb interaction, and, the tunneling-induced symmetric-antisymmetric single-particle gap, on the nature of the DQW ground state. [The three energy scales are related to the three important length scales in the problem: The magnetic length (l_c), the interwell separation (d), and, the thickness of each layer (λ), which, in turn, are determined by the sample parameters V_w, V_b, D_w, D_b, and, the applied magnetic field B.] Wherever possible, we have compared our results with the existing experimental data[25,26,29,35] on FQHE in DQW systems. In general, both qualitative and quantitative agreement between our theory and experimental results is very good. We have also made experimentally verifiable predictions about the phase diagram of DQW quantum Hall states as a function of system parameters.

We have considered only the lowest spin-split state in the lowest Landau level, neglecting Landau-level coupling and assuming complete spin polarization. We also consider only the balanced situation where the two wells are identical and the average occupancy in each well is the same, namely, $\nu/2$. While the experiments[25,26,29] we are primarily interested in satisfy these conditions, relaxing these conditions (i.e., having unequal electron densities in the two wells, including Landau-level coupling, and considering both the spin states) should lead to a rich and complex DQW phase diagram consisting of many different FQH states. Considering systems with more than two layers should also lead to many interesting possibilities. Our theoretical technique of using finite-size spherical diagonalization, while being a well-established and well-tested numerical method for studying FQHE, does suffer from the usual problem of any small-system simulation. The results should be taken with some caution, but we believe that our finite-size calculations are qualitatively reliable and well suited for pedicting the various incompressible states in the DQW systems studied in this paper and recently observed experimentally.

The three filling factors $\nu=\frac{1}{2}$, $\frac{2}{3}$, and 1 considered by us in this article have the following qualitative difference. The $\nu=\frac{1}{2}$ state is compressible both in the $d\rightarrow 0$ and the $d\rightarrow\infty$ limit, because neither single 2D layers with $\nu=\frac{1}{2}$ (i.e., the $d=0$ limit), or, two isolated 2D layers, each with $\nu=\frac{1}{4}$ (i.e., the $d=\infty$ limit), exhibit no FQHE. On the other hand, for intermediate values of the layer separation d, the $\nu=\frac{1}{2}$ DQW system does have an incompressible FQH state which is stable over a finite range of d/l_c where the competition between intrawell and interwell Coulomb correlation energies produces the 331 many-body ground state[4] of Halperin. The $\nu=1$ state in a DQW, on the other hand, is the incompressible regular

IQHE state (the $\Psi^{(s)}_{\nu=1}$ state) in the $d\to 0$ limit (corresponding to one completely filled Landau level in a 2D layer), whereas in the $d\to\infty$ limit, the ground state must be compressible with no QHE because it corresponds to two isolated 2D layers, each with $\nu=\frac{1}{2}$ occupancy. For intermediate values of d, however, our theoretical calculations suggest that the $\nu=1$ DQW system may, for suitable values of d and Δ_{sas}, acquire an incompressible ground state Ψ_{111} which is stabilized by the interwell Coulomb interaction. Finally, the $\nu=\frac{2}{3}$ DQW state is different from both the $\nu=\frac{1}{2}$ and $\nu=1$ states, because it is incompressible in both the $d\to 0$ limit (the $\Psi^{(s)}_{\nu=2/3}$ state) and the $d\to\infty$ limit (the Ψ_{330} state). The $\nu=\frac{2}{3}$ DQW system, according to our calculations, shows FQHE for all values of d, going directly from the $\Psi^{(s)}_{\nu=2/3}$ incompressible state to the Ψ_{330} incompressible state at some finite value of d/l_c where the interwell Coulomb interaction energy overcomes the Δ_{sas} tunneling gap.

Thus, schematically we may represent the university class of various possible ground states (as a function of increasing d or decreasing Δ_{sas}, keeping all other parameters, viz. l_c and λ, fixed) in the following way:

	$d=0\longrightarrow$	d/l_c finite $\longrightarrow$	$d=\infty$
$\nu=\frac{1}{2}$	Compressible $\longrightarrow$	Incompressible $\longrightarrow$	Compressible
$\nu=1$	Incompressible $\longrightarrow$ ($\Psi^{(s)}_{\nu=1}$)	Compressible ↓	
		[Incompressible] $\longrightarrow$ (Ψ_{111})	Compressible
$\nu=\frac{2}{3}$	Incompressible ($\Psi^{(s)}_{\nu=2/3}$)	$\longrightarrow$	Incompressible (Ψ_{330})

The incompressible many-body Ψ_{111} state at $\nu=1$ is not accessible for all values of the well parameter, as is obvious from the phase diagram of Fig. 15. Clearly, under suitable conditions there is a very interesting possibility of a reentrant $\nu=1$ QHE in a DQW structure as a function of Δ_{sas} (or d/l_c) where one goes from the $\Psi^{(s)}_{\nu=1}$ ground state to the Ψ_{111} state via a compressible non-QH state in between. The search for this reentrant behavior should be carried out in samples with small values of d by varying an in-plane magnetic field which can drastically suppress[29] interlayer tunneling, making it possible to go along a horizontal line in Fig. 15 where the transitions $\nu=1$ (IQHE), $\psi^{(s)}_{\nu=1}\to$compressible $\to\nu=1$ (FQHE), Ψ_{111} should be observable. The Ψ_{111} state would, in general, have a lower activation energy than the $\Psi^{(s)}_{\nu=1}$ state, and, the compressible state in between obviously would not exhibit any QHE.

The fact that incompressibility would be destroyed with increasing layer separation (in a $\nu=1$ DQW system) was first pointed out[36] by Fertig on the basis of a single-mode calculation. The indication for a possible many-body $\nu=1$ QHE in the $\Delta_{sas}=0$ situation in DQW structures was first obtained in Ref. 22 via finite-size numerical calculations on a rectangular geometry (no contact with the Ψ_{111} state was, however, made in Ref. 22). There have recently been some attempts[37,38] at elucidating the nature of the compressible state the system goes into when the $\nu=1$ (or, $\nu=\frac{1}{2}$) QHE (i.e., the incompressibility) is destroyed by Coulomb interactions. Based on Hartree-Fock calculations,[37,38] it has been suggested that these compressible states (for example, the region outside the two solid lines in our Fig. 15 where the state is neither the $\Psi^{(s)}_{\nu=1}$ state nor the Ψ_{111} state and is a compressible state with no excitation gap in our numerical calculation) are actually charge-density-wave states. We disagree with these suggestions[37,38] and believe that the compressible states the DQW system goes into at finite well separations are ordinary even-denominator (i.e., $\nu=\frac{1}{4}$ or $\frac{1}{2}$ states in single-layer systems) liquid compressible states[39] where the 2D charge density in each layer is uniform. In fact, we believe that only when the average occupancy ($\nu/2$) in each individual layer is quite low ($\nu/2\lesssim 1/5$) does one expect to see charge-density-wave or Wigner-crystal-type states in DQW systems—the situation should not be too different from a single-layer system[40] where only for $\nu\lesssim 1/7$, a charge-density-wave or Wigner-crystal-type state is energetically favorable over a liquid state. The presence of a second layer may help the formation of a charge density wave to some extent by increasing somewhat the value of the critical ν ($\lesssim 2/7$) for the instability but $\nu=1$ and $\frac{1}{2}$ states, in our opinion, are unlikely to be charge-density-wave states. Our numerical results are consistent with these conclusions—we find, for $\nu=1$ and $\frac{1}{2}$, the compressible states to have uniform charge density in each layer, indicating that they are *not* charge-density-wave states, but are most likely strongly renormalized Fermi-liquid-type states.[41] We have numerically calculated the pair-correlation function for the $\nu=1$ situation corresponding to our Fig. 15, finding it to be qualitatively the same in all parts of our phase diagram, indicating that the compressible state for large d/l_c are liquid states. We believe that Hartree-Fock calculations[37,38] which, in the absence of any kinetic energy (i.e., the lowest Landau-level approximation) *always* predict charge-density-wave-type ground states, are not reliable for $\nu=1$, $\frac{2}{3}$, $\frac{1}{2}$ states considered in this paper where Laughlin-type correlations, not included in the Hartree-Fock theory, are dominant. We believe that the various transitions between ground states in the DQW structures which occur as some parameter (d or l_c or Δ_{sas}) is varied are all first-order transitions driven by energy differences between various compressible and incompressible ground

states. These transitions occur abruptly at some sharp values of the system parameters as a particular ground state is lowered in energy compared with some other due to the competition among intrawell and interwell correlation energies and the symmetric-antisymmetric gap energy associated with single-particle tunneling effect.

We conclude by summarizing what we believe to be the important highlights of the theoretical results presented in this paper. We have shown that, at least within the numerical limitations of a finite-size exact diagonalization calculation on spheres, the $\nu=\frac{1}{2}$ FQHE recently observed[25,26] in DQW structures by two different groups belong to the same universality class and are both due to the stabilization of Halperin's[4] 331 incompressible ground state by interwell Coulomb correlation effects. This is true for Ref. 26 even in the presence of substantial interwell tunneling effects because the 331 state, as is true for Laughlin-type correlated wave functions in general, is robust, and remains the ground state of the system over a range of values of system parameters and, also because the bare tunneling gap is substantially renormalized by Coulomb interaction. Our calculated excitation gaps and the predicted values of l_c where the $\nu=\frac{1}{2}$ FQHE is stable (i.e., the values of l_c where the overlap between the 331 state and the numerical ground state is high) agree with the experimental results.[25,26] We have also shown that the $\nu=1$ QHE observed in Refs. 25 and 26 actually belong to different universality classes[42]—in Ref. 26, one sees the $\Delta_{\rm sas}$ stabilized single-particle QHE whereas in Ref. 25 one sees the many-body Ψ_{111} ground state which is being stabilized by interwell correlation energy. We have obtained the phase diagram for the $\nu=1$ situation in a DQW structure, where three different phases are possible depending on the relative values of d/l_c and $\Delta_{\rm sas}/(e^2/\varepsilon l_c)$—for large $\Delta_{\rm sas}$ one has the $\psi^{(s)}_{\nu=1}$ ground state with the $\nu=1$ IQHE (this is the situation in Ref. 26), for small $\Delta_{\rm sas}$ and $d/l_c \lesssim 1$, it is possible to have the many-body Ψ_{111} ground state with the $\nu=1$ "FQHE". For large d/l_c, we find compressible states at $\nu=1$ which exhibit no QHE. One interesting feature of our phase diagram is the prediction of a reentrant $\nu=1$ QHE in DQW structures as a function of decreasing $\Delta_{\rm sas}$ where one should first see the destruction of the QHE at $\nu=1$ as the system undergoes a phase transition from the $\Psi^{(s)}_{\nu=1}$ ground state to a compressible ground state, and, then at small $\Delta_{\rm sas}$ (but, for fixed $d/l_c \lesssim 1$), the QHE at $\nu=1$ should reappear as the system makes a phase transition from the compressible state to the many-body Ψ_{111} state. (Experimentally, one can change $\Delta_{\rm sas}$ at a fixed d/l_c by applying a small in-plane magnetic field.) It would be interesting to experimentally observe this nontrivial reentrant behavior. At $\nu=\frac{2}{3}$, we predict a quantum phase tansition in the DQW structure where, at some finite and sharp values of d/l_c, the system goes directly from one type of incompressible ground state ($\Psi^{(s)}_{\nu=2/3}$) to another (Ψ_{330}) with a concomitant abrupt change in the activation energy. This should also be experimentally observable according to our finite-size numerical calculations. The various quantum phase tansitions between different compressible and incompressible states at $\nu=1$, $\frac{2}{3}$, and $\frac{1}{2}$ discussed in this paper are all direct first-order transitions driven by the competition between intrawell and interwell Coulomb interactions, and, the interwell tunneling gap.

ACKNOWLEDGMENTS

The authors acknowledge helpful conversations with J.P. Eisenstein, G. S. Boebinger, F. D. M. Haldane, X. G. Wen, M. Shayegan, and A. H. MacDonald. This work is supported by the National Science Foundation Materials Theory (DMR) Program (at Maryland) and the Physics Program (at Santa Barbara). One of the authors (S.D.S.) acknowledges the hospitality of the staff of the Institute for Theoretical Physics at the University of California, Santa Barbara.

*Present and permanent address: AT&T Bell Laboratories, Murray Hill, NJ 07974.
†Present and permanent address.
‡Present and permanent address: Department of Physics, Oklahoma State University, Stillwater, OK 74078.

[1]R. B. Laughlin, Phys. Rev. Lett. **50**, 1395 (1983).
[2]D. C. Tsui, H. L. Störmer, and A. C. Gossard, Phys. Rev. Lett. **48**, 1559 (1982).
[3]*The Quantum Hall Effect,* edited by R. E. Prange and S. M. Girvin (Springer, New York, 1990).
[4]B. I. Halperin, Helv. Phys. Acta. **56**, 775 (1963).
[5]F. D. M. Haldane, Phys. Rev. Lett. **51**, 605 (1983).
[6]B. I. Halperin, Phys. Rev. Lett. **52**, 1583 (1984).
[7]J. K. Jain, Phys. Rev. B **41**, 7653 (1990).
[8]K. von Klitzing, G. Dorda, and M. Pepper, Phys. Rev. Lett. **45**, 494 (1980).
[9]F. C. Zhang and T. Chakraborty, Phys. Rev. B **34**, 7076 (1986); P. A. Maksym, J. Phys. Condens. Mat. **1**, L6299 (1989); X. C. Xie, Y. Guo, and F. C. Zhang, Phys. Rev. B **40**, 3487 (1989).
[10]F. D. M. Haldane and E. H. Rezayi, Phys. Rev. Lett. **60**, 956 (1988).
[11]A. H. MacDonald, D. Yoshioka, and S. M. Girvin, Phys. Rev. B 8044 (1989).
[12]R. Willett, J. P. Eisenstein, H. L. Störmer, D. C. Tsui, A. C. Gossard, and J. H. English, Phys. Rev. Lett. **59**, 1776 (1987).
[13]R. G. Clark, S. R. Haynes, A. M. Suckling, J. R. Mallett, J. J. Harris, and C. T. Foxon, Phys. Rev. Lett. **62**, 1536 (1989); J. P. Eisenstein, H. L. Störmer, L. Pfeiffer, and K. W. West, *ibid.* **62**, 1540 (1989).
[14]S. Das Sarma and A. Madhukar, Phys. Rev. B **23**, 805 (1981); J. K. Jain and S. Das Sarma, *ibid.* **36**, 5949 (1987); Surf. Sci. **196**, 466 (1988).
[15]A. Pinczuk, M. G. Lamont, and A. C. Gossard, Phys. Rev. Lett. **56**, 2092 (1986); G. Fasol, N. Mestres, H. P. Hughes, A. Fischer, and K. Ploog, *ibid.* **56**, 2517 (1986).
[16]F. D. M. Haldane and E. H. Rezayi, Bul. Am. Phys. Soc. **32**, 892 (1987).
[17]S. Das Sarma and R. E. Prange, Science **256**, 1284 (1992).
[18]F. C. Zhang and S. Das Sarma, Phys. Rev. B **53**, 2093 (1986).
[19]S. He, F. C. Zhang, X. C. Xie, and S. Das Sarma, Phys. Rev. B **42**, 11 376 (1990).
[20]M. Shayegan, J. Jo, Y. W. Suen, M. Santos, and V. J. Gold-

man, Phys. Rev. Lett. **65**, 2916 (1990).
[21]D. Yoshioka, A. H. MacDonald, and S. M. Girvin, Phys. Rev. B **39**, 1932 (1989).
[22]T. Chakraborty and P. Pietiläinen, Phys. Rev. Lett. **59**, 2784 (1987).
[23]Song He, X. C. Xie, S. Das Sarma, and F. C. Zhang, Phys. Rev. B **43**, 9339 (1991); Song He, X. C. Xie, and S. Das Sarma, Surf. Sci. **263**, 87 (1992).
[24]Song He, PhD thesis, University of Maryland (1991).
[25]J. P. Eisenstein, G. S. Boebinger, L. N. Pfeiffer, K. W. West, and Song He, Phys. Rev. Lett. **68**, 1383 (1992).
[26]Y. W. Suen, L. W. Engel, M. B. Santos, M. Shayegan, and D. C. Tsui, Phys. Rev. Lett. **68**, 1379 (1992).
[27]M. P. Stopa and S. Das Sarma, Phys. Rev. B **45**, 8526 (1992).
[28]M. Greiter, X. G. Wen, and F. Wilczek, Phys. Rev. B **46**, 9586 (1992).
[29]G. S. Boebinger, H. W. Jiang, L. N. Pfeiffer, and K. W. West, Phys. Rev. Lett. **64**, 1793 (1990).
[30]A. H. MacDonald, P. M. Platzman, and G. S. Boebinger, Phys. Rev. Lett. **65**, 775 (1990).
[31]A. H. MacDonald, Surf. Sci. **229**, 1 (1990).
[32]F. D. M. Haldane, in *The Quantum Hall Effect* (Ref. 3), Chap. 8; F. D. M. Haldane and E. H. Rezayi, Phys. Rev. Lett. **54**, 237 (1985).
[33]G. Fano, F. Ortolani, and E. Colombo, Phys. Rev. B **34**, 2670 (1986).
[34]S. M. Girvin, in *The Quantum Hall Effect* (Ref. 3), Chap. 9.
[35]J. P. Eisenstein (private communication).
[36]H. A. Fertig, Phys. Rev. B **40**, 1087 (1989).
[37]L. Brey, Phys. Rev. Lett. **65**, 903 (1990).
[38]X. M. Chen and J. J. Quinn, Phys. Rev. Lett. **67**, 895 (1991).
[39]G. Fano, F. Ortolani, and E. Tossatti, Nuovo Cimento **9D**, 1337 (1987).
[40]P. K. Lam and S. M. Girvin, Phys. Rev. B **30**, 473 (1984).
[41]B. I. Halperin, P. A. Lee, and N. Read, Phys. Rev. B (to be published).
[42]We mention that if the quantum states are classified *only* by their total pseudospins, then the $\Psi^{(s)}_{\nu=1}$ state and the Ψ_{111} state do *not* belong to different universality classes because they both have the same total pseudospin $S=(N-1)/2$ which means that they belong to the same irreducible representation of the total pseudospin. (Their pseudospins are rotated with respect to each other with the Ψ_{111} state having its pseudospin pointing in the y direction and the $\Psi^{(s)}_{\nu=1}$ state having its pseudospin along the x direction.) On the other hand, physically these two states are quite different, particulary in terms of the elementary excitations which determine their thermodynamic properties. For example, in the absence of any interwell tunneling, the Ψ_{111} state will have a gapless collective mode due to the broken symmetry in the pseudospin x-y plane whereas the $\Psi^{(s)}_{\nu=1}$ state *always* has a finite energy gap. Thus, the system is in *different thermodynamic* phases in these two cases even if they belong to the same irreducible pseudospin representation. In the presence of weak interwell tunneling, an energy gap proportional to the square root of the tunneling strength will open up in the Ψ_{111} state, and again, the activation energies for the two states will be quite different. Therefore, the different universality classes (and the quantum phase transitions between them) being discussed here are *not* defined by the total pseudospin, but by the thermodynamic behavior of the two phases. The same consideration applies to the $\nu=\frac{2}{3}$ situation for the $\Psi^{(s)}_{\nu=2/3}$ and the Ψ_{330} states.